

Article

Physical Drivers and Dominant Oceanographic Processes on the Uruguayan Margin (Southwestern Atlantic): A Review and a Conceptual Model

Leticia Burone ^{1,*}, Paula Franco-Fraguas ¹, Alvar Carranza ², Danilo Calliari ³, Michel Michaelovitch de Mahiques ⁴ , Mónica Gómez ¹ , Yamandú Marin ¹ , Ofelia Gutiérrez ⁵ and Leonardo Ortega ⁶

- ¹ CINCYTEMA, Sección Oceanología, Instituto de Ecología y Ciencias Ambientales, Facultad de Ciencias, Universidad de la República, Iguá 4225, Montevideo 11400, Uruguay; paulafrancof@gmail.com (P.F.-F.); mge@fcien.edu.uy (M.G.); ymarin.ltp@gmail.com (Y.M.)
 - ² Centro Universitario Regional Este (CURE) Sede Maldonado, Universidad de la República, Maldonado 21000, Uruguay; alvar.carranza@gmail.com
 - ³ Oceanografía y Ecología Marina, Instituto de Ecología y Ciencias Ambientales, Facultad de Ciencias, Universidad de la República, Iguá 4225, Montevideo 11400, Uruguay; danilocalliari@gmail.com
 - ⁴ Instituto Oceanográfico da Universidade de São Paulo, Praça do Oceanográfico, 191, São Paulo 05508-120, Brazil; mahiques@usp.br
 - ⁵ UNICIEP, Instituto de Ecología y Ciencias Ambientales, Facultad de Ciencias, Universidad de la República, Iguá 4225, Montevideo 11400, Uruguay; oguti@fcien.edu.uy
 - ⁶ Sección Oceanografía, Departamento de Biología Pesquera, Dirección Nacional de Recursos Acuáticos (DINARA), Ministerio de Ganadería Agricultura y Pesca, Constituyente 1497, Montevideo 11200, Uruguay; lortega@dinara.gub.uy
- * Correspondence: lburone@fcien.edu.uy



Citation: Burone, L.; Franco-Fraguas, P.; Carranza, A.; Calliari, D.; Michaelovitch de Mahiques, M.; Gómez, M.; Marin, Y.; Gutiérrez, O.; Ortega, L. Physical Drivers and Dominant Oceanographic Processes on the Uruguayan Margin (Southwestern Atlantic): A Review and a Conceptual Model. *J. Mar. Sci. Eng.* **2021**, *9*, 304. <https://doi.org/10.3390/jmse9030304>

Academic Editor: Jorge Guillén

Received: 7 December 2020

Accepted: 1 March 2021

Published: 9 March 2021

Publisher's Note: MDPI stays neutral with regard to jurisdictional claims in published maps and institutional affiliations.



Copyright: © 2021 by the authors. Licensee MDPI, Basel, Switzerland. This article is an open access article distributed under the terms and conditions of the Creative Commons Attribution (CC BY) license (<https://creativecommons.org/licenses/by/4.0/>).

Abstract: The Uruguayan continental margin (UCM), located in the Southwestern Atlantic margin's subtropical region, is positioned in a critical transitional region regarding the global ocean circulation (Río de la Plata (RdIP) outflow and Brazil-Malvinas Confluence), as also reflected in seafloor features (northernmost distribution of a large depositional contourite system and RdIP paleovalley). This complex oceanographic scenario occurring in a relatively small area highlights the advantage of considering the UCM as a natural laboratory for oceanographic research. The present work provides the first conceptual "control" model of the physical drivers (i.e., climate, geomorphology) and main oceanographic processes (i.e., hydrodynamics, sediment, and carbon dynamics) occurring along the UCM, reviewing and synthesizing available relevant information based on a functional integrated approach. Despite the conspicuous knowledge gaps on critical processes, a general picture of the system's functioning is emerging for this complex biophysical setting. This includes conceptualizations of the actual controls, main processes, feedbacks, and interactions responsible for system dynamics. The structure adopted for developing our conceptual models allows permanent improvement by empirical testing of the working hypothesis and incorporating new information as scientific knowledge advances. These models can be used as a baseline for developing quantitative models and, as representations of relatively "pristine" conditions, for stressors models by identifying sources of stress and ecological responses of key system attributes under a transboundary approach.

Keywords: Uruguayan margin; Southwestern Atlantic; conceptual models

1. Introduction

1.1. Continental Margins

Continental margins, the area that encompasses the continental shelf, slope, and rise [1], comprise a significant portion (11–20%) of oceanic area [2–4]. These are dynamic, heterogeneous environments shaped by tectonic, atmospheric, terrestrial, and oceanic influences [5]. Continental margins provide invaluable food and energy resources and perform

essential functions such as carbon and nutrient cycling. Concerning the total biosphere active carbon cycling in less than 10,000 y (40,000 gigatons), ca. 95% of this flux ($\sim 38,000 \text{ Gt C}$) is stored in the ocean as dissolved inorganic carbon (DIC), and one of the main processes transforming DIC into organic carbon in the marine realm is photosynthesis [6]. Approximately half of the world's net annual photosynthesis occurs in the oceans ($\sim 48 \text{ Pg C y}^{-1}$), and the continental margins support 10–15% of this production [7]. More than 90% of all organic carbon burial [4] and 32% of the biogenic silica deposition [3] occurs in these areas, which constitute a variable but increasing global sink for human-generated carbon dioxide (e.g., [8]). Continental margins thus provide essential ecosystem functions and services, also harboring non-renewable resources. Thus, a wealth of resources, including deep-water fish stocks, an enormous bioprospecting potential, and elements and energy reserves, are currently being utilized and prospected and surely face increasing attention soon.

Further, continental margins operate as libraries recording the history of macro-, meso-, and micro-scale processes operating at geological and ecological timescales, such as continental drift and the genesis of oceans, the geological history of Earth, climatic and oceanographic changes (e.g., [9]), the global carbon cycle [10], and other biogeochemical cycles involving material and energetic fluxes in marine ecosystems [11]. Due to this complexity, significant information gaps arise regarding the roles and functions of these areas and their consequences on the functioning of the whole Earth system [12]. Thus, the identification, quantification, and modeling of these roles will allow us to develop scenarios of natural conditions and potential changes under the anthropogenic influence, constituting scientific challenges that must be addressed in an interdisciplinary way.

The present work aims to provide a conceptual model of the main physical drivers and the oceanographic processes (i.e., hydrodynamics, sediment, and carbon dynamics) occurring along the Uruguayan continental margin (UCM), reviewing and synthesizing available relevant information based on a functional integrated approach. This approach includes the development of the first conceptual “control” models of the UCM. Also, their relationship with selected biological components of the system is considered. These models represent relatively “pristine” conditions rather than depicting the functioning of an impacted or degraded system. They are expected to fuel the development of further improvements on the conceptual model incorporating multiple “stressors,” also adjusting the “control” models by empirical testing of working hypothesis, reviewing current information, and incorporating new information as scientific knowledge advances.

1.2. The Uruguayan Continental Margin on a Global and Local Scale

The Uruguayan continental margin (UCM) is located in the subtropical region (i.e., between 33° S and 38° S) of the Southwestern Atlantic margin, positioned in a key transitional region concerning global ocean circulation, and is part of the Southeast South American Shelf Large Marine Ecosystem (LME). Furthermore, from a global perspective for marine conservation planning, this area is also classified as the Uruguay–Buenos Aires shelf ecoregion (Marine Ecoregion of the World, MEOW N°183). The global and hierarchical nature of the LMEs and MEOW in this ecoregion can support analytical approaches that move between scales, especially because of its high biodiversity and for sustaining a number of economic activities, including commercial fisheries, tourism, and maritime transportation. Likewise, categorization into the Pelagic Provinces of the World (PPOW) scheme, the UCM is located in the Malvinas Current Province. This province is a large epipelagic area of the Atlantic Ocean defined by large-scale, spatially and temporally stable (or seasonally recurrent) oceanographic drivers.

Hydrodynamics in the UCM is strongly influenced by the Río de la Plata (RdIP) outflow, the second river basin in South America (discharge estimated at $23,000 \text{ m}^3 \text{ s}^{-1}$ during 1931–2016), although this value has increased to $25,000 \text{ m}^3 \text{ s}^{-1}$ during the past few decades (1997–2016) [13,14]; and by the encounter of subtropical and subantarctic water masses, transported by the Brazil and Malvinas currents, worldwide known as the Brazil–Malvinas Confluence (BMC; Figure 1B). High marine productivity characterizes this

system [15], controlled by the high-pressure systems of the Pacific Ocean and South Atlantic Ocean. At a closer look, the UCM contains practically all types of marine fronts described in the literature. These include the estuarine (salinity) front, plume front, upwelling front, shelf-break front, fronts associated with the convergence and divergence of water masses, and fronts associated with submarine canyons [16–19].

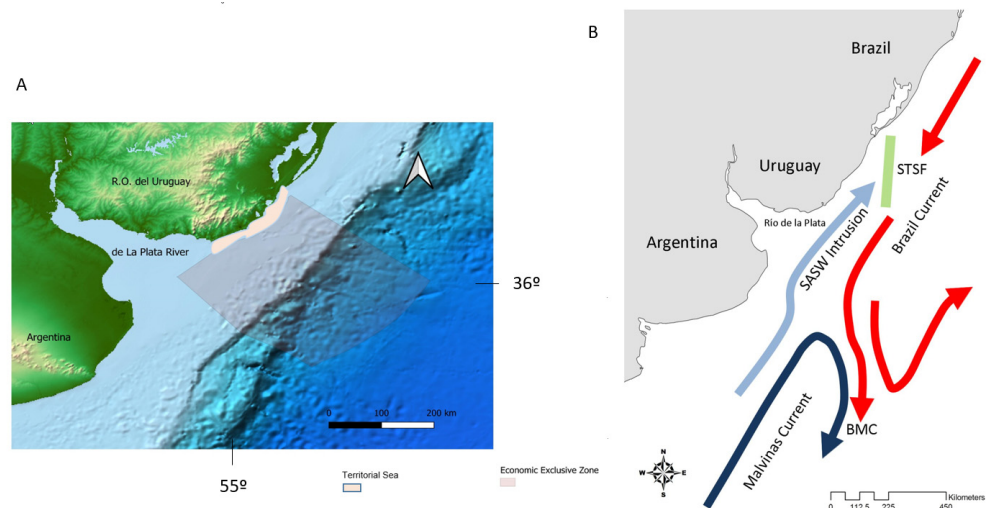


Figure 1. Map showing the location of the study area; the Territorial Sea and the Economic Exclusive Zone are indicated (A); schematic representation of the regional circulation of the Southwestern Atlantic continental shelf and slope, redrawn from Matano et al. (2010); (B) Subantarctic Shelf Water (SASW), Subtropical Shelf Front (STSF), Brazil–Malvinas Confluence (BMC).

The transitional character and complex hydrodynamics of the UCM are also imprinted on the seafloor and include the northernmost distribution of an enormous contouritic depositional system (CDS; depositional, erosional, and mixed features formed by bottom currents). The CDS in the UCM was delineated by the continuous action of Antarctic water masses along the Pleistocene. It also presents the RdIP Pleistocene drain imprint (paleovalley and mud belts [20–24] (Figures 1A and 2).

Structure of Conceptual Models

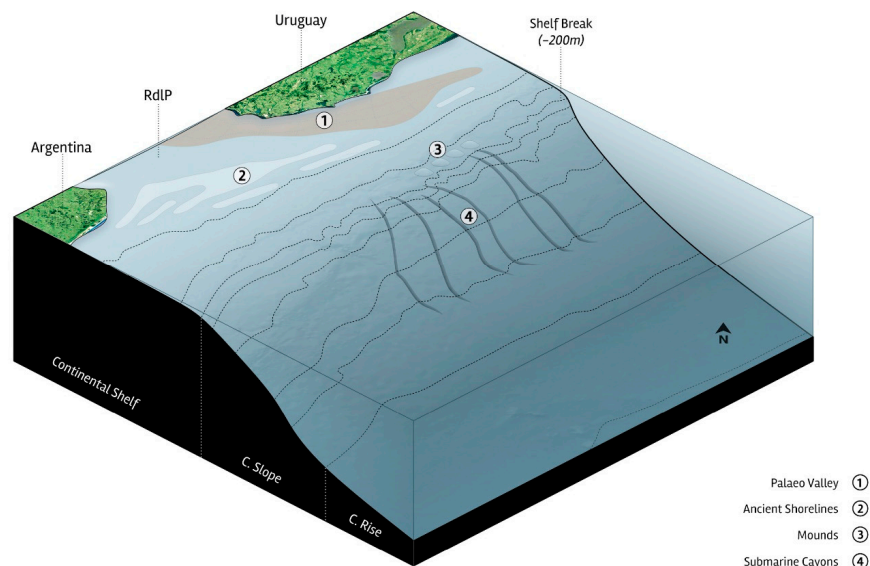


Figure 2. Schematic representation of the horizontal subdivision (subsystems) of the continental margin showing general geomorphological characteristics.

Such a conspicuous oceanographic scenario occurs in a relatively small area (around 184,000 km²; Figure 1A) and highlights the advantage of considering the UCM as a natural laboratory for oceanographic research. However, knowledge of UCM oceanographic processes is still scarce and dispersed, and little is known about oceanographic processes from an integrated perspective [21,25,26]. This lack of knowledge poses an additional issue towards the sustainable management of UCM, also impairing international research efforts.

Coastal and offshore waters off Uruguay have been used for maritime commerce, exploration, fisheries, transportation, and military purposes for over 400 years, due to the excellent natural port (Montevideo Port), connecting with the RdIP and inland national and regional waterways. Tourism and services are the main economic activity associated with the coastline and fishing activities (ports and navigation channels also use the coastline). Within the Uruguayan Exclusive Economic Zone (U-EEZ), fishing activity represents 0.12% of the Gross Domestic Product (GDP) annually and 3.4% of the total Uruguayan exports, while tourism (mainly attracted by coastal “beach and sun” recreational activities) accounts for 7% (DIEA, 2018 in www.presidencia.gob.uy, accessed on 5 March 2021). Though historically discontinuous and limited, offshore oil and gas exploration in Uruguay has increased in the last years, and submarine communications cables were also deployed in the seabed [27]. Despite this, marine protected areas (MPAs) coverage accounts for 0.23% (416.5 km²), and current management programs could be significantly improved.

1.3. Conceptual Models as Tools for Integrated Marine Management

Conceptual models (CM) express ideas about components and processes deemed necessary in a system, document assumptions about how components and processes are related, and identify knowledge gaps. They are working hypotheses about system form and function [28], and thus there is not a single “correct” CM [29]. These models are key elements of environmental monitoring programs because they provide a broad but synthesized scientific framework of the system dynamics. They also help communicate the interactions between systems components, thus justifying the choice of indicators used in monitoring programs [30]. In general, two different model structures are used: the “control” and the “stressor” models [30]. The former are conceptualizations of the actual controls, main processes, feedbacks, and interactions responsible for system dynamics and, hence, need to be represented mechanistically. They represent the first steps for the development of stressors models [30]. On the other hand, stressor models are intended to illustrate sources of stress and the ecological responses of key system attributes. In the present work, CM conceptualization is intended to represent the baseline for the future development of stressor models, which will be taken into account when implementing management measures. It should be noted that the entire RdIP and the adjacent Atlantic Ocean is also a common water space under a transboundary management scheme between Argentina and Uruguay through the Río de la Plata and its Maritime Front Treaty (1973). The Parties shall establish a Binational Technical Commission, charged with research and the adoption and coordination of plans and measures concerning the conservation, preservation, and rational exploitation of living resources and protection of the marine environment in the common interest zone.

2. Environmental Context

2.1. Ocean–Atmosphere Coupling and Water Masses

The poleward heat transport is controlled by the atmosphere and ocean circulations. Ocean–atmosphere coupling is a significant cause of climate variability; this system promotes the atmosphere’s influence on the ocean and vice versa.

The South Atlantic Subtropical Gyre encompasses a system of wind-driven surface currents [31] and dominates the South Atlantic Ocean’s surface circulation. The gyre circulation is counter-clockwise, and its position in the Atlantic basin depends on the Southern Hemisphere’s general wind patterns. It is formed by the southward flowing western boundary Brazil Current (BC), which flows along the South American coast then

meets the northeastward extension of the Antarctic Circumpolar Current (ACC) into the Atlantic, the Malvinas Current, resulting in the Brazil–Malvinas Confluence [32]. The eastward flow originates as the South Atlantic Current (SAC) [33], the subtropical gyre’s southern branch. Part of the SAC incorporates in the Benguela Current (BeC) to the north, which marks the eastern boundary of the subtropical gyre. The BeC then flows northwestward and turns into the South Equatorial Current (SEC) southern branch, forming the subtropical gyre’s northern boundary [34,35]. The westward flowing SEC advects subtropical waters toward the Brazilian shelf region, where it bifurcates at approximately 15° S, closing the subtropical gyre by flowing into the southward BC [33]. Water masses transported by the BC and MC enter the continental shelf along the Brazilian Basin and Patagonia shelf break, respectively. Subtropical Shelf Waters (STSW) and Subantarctic Shelf Waters (SASW) are displaced southward and northward, respectively, along the continental shelf then diluted by the continental runoff of the RdIP and the Patos Lagoon (Brazil). These water masses’ confluence generates the Subtropical Shelf Front (STSF), presumably detached offshore [17]. Consequently, the STSF is considered a critical component of the oceanographic process that connects the Southwestern Atlantic Shelf to the deep ocean [17].

Surface water masses (0–500 m) in the UCM are Tropical Water (TW) and South Atlantic Central Water (SACW) [36], both with a southward net transport as a part of the BC. SACW formation occurs in the BC and MC confluence zone [37] and recirculates within the southern subtropical gyre. These water masses are warm and salty compared to the Subantarctic Water and Antarctic Intermediate Water (AAIW) from the Malvinas Current with a net northward transport. At about 1200 m depth, Upper Circumpolar Deep Water (UCDW) shows a net northward transport. Below this, the North Atlantic Deep Water (NADW) that constitutes the principal source of ocean ventilation below the thermocline shows a southward net transport and is underneath the Upper Circumpolar Deep Water. Below the NADW is the Lower Circumpolar Deep Water (LCDW), and below 4000 m, the abyssal circulation is dominated by the Antarctic Bottom Water (AABW) [31] (Figure 3).

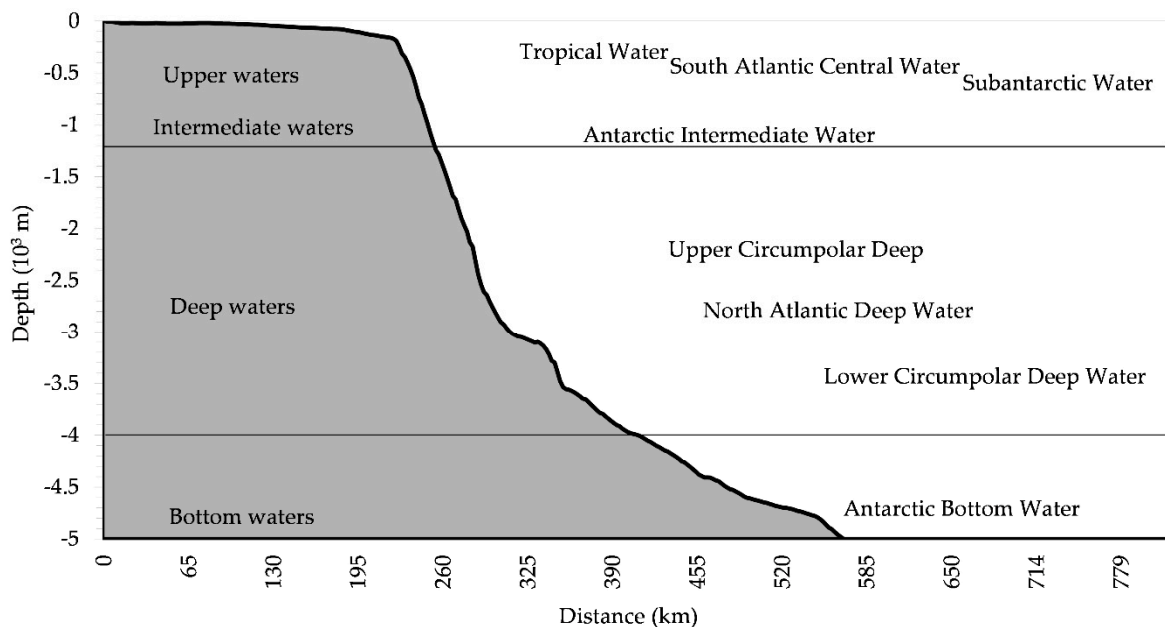


Figure 3. Simplified oceanographic profile with the bathymetric distribution of the different water masses along the Uruguayan continental margin.

Surface temperature and salinity distributions in the region are controlled by local atmospheric conditions and remotely by regional and global-scale climate variability modes ([38] e.g., El Niño–Southern Oscillation). Large amplitude variations in continental runoff and low-level winds at seasonal and interannual time scales induce significant changes

in shelf water masses [39] and the shelf-deep ocean exchanges [40]. The variations in RdIP discharge modulates the input and distribution of freshwater and nutrients, which lead to significant changes in water mass properties over the continental shelf [41,42] and impact the sediment and nutrient load over the continental shelf and offshore areas [43]. Thus, continental runoff variability driven by atmospheric surface circulation regulates the water mass characteristics in the outer estuary and over the shelf. These atmospheric forcing and river discharge change substantially impact the location of fronts' positions and water column properties [44]. The sensitivity of the South West Atlantic Ocean (SWAO) shelf circulation to changes in wind pattern is higher in UCM's neighbor. Seasonal reversals of the shelf circulation occur in this region in response to along-shelf wind patterns, from southwesterly in austral fall–winter to northeasterly in spring–summer [45]. These seasonal reversals in the shelf circulation induce a northeastward extension of the low-salinity/high-nutrient Río de la Plata Plume (RPP) and its southwestward retreat in spring–summer [18,46]. Variations of the Southwestern Atlantic marine circulation patterns and the sea surface temperature (SST) occur over time scales ranging from sub-seasonal to seasonal to interannual. These variations are influenced by the interactions between the opposite flows of the Brazil Current (BC) and the Malvinas Current (MC), which in turn are affected by the basin wind field and other atmospheric characteristics, such as the South Atlantic Convergence Zone (SACZ) [40]. The SACZ extends south-eastward from the center of the South American continent to the South Atlantic [41,42] and is generated by moisture convergence between the South Atlantic high pressure and the continental thermal low-pressure zones [43]. Still, the oceanic part is strongly dependent on the convergence of the low-level southern moisture flow [42]. The high-pressure center in the Atlantic Ocean shifts according to natural seasonal cycles and determines the distribution of ocean currents that displace the subtropical and subantarctic water masses, also influencing the RPP. Precipitation is associated with the low-pressure center located on the continent. During El Niño–Southern Oscillation (ENSO) warm phase, precipitation increases considerably during austral spring and summer, augmenting the RdIP flow.

2.2. Geomorphologic Characterization

The continental margin of the South Atlantic Margin is a typical passive margin characterized by an extensive continental shelf that widens to the south. This margin was developed during the Atlantic Ocean formation during the Upper Cretaceous [47,48]. The UCM is described as a segmented, volcanic rifted margin [49,50]. The origin of the sediment fill that forms the UCM originates in the Dom Feliciano Belt (called Sierra del Este in the E of Uruguay), raised before the early Cretaceous, before the breakup of the supercontinent Pangea and the opening of the South Atlantic Ocean [50,51]. Two main basins are recognized offshore Uruguay, with a distinct Mesozoic and Cenozoic evolution; the Punta del Este Basin to the south, and the Pelotas Basin or Laguna Merín Tectonic Basin to the north [49]. These are separated in the shelf shallow waters by a basement high, the so-called Polonio High.

The morphology and sedimentary covertures of the UCM reflect the global climatic and oceanographic changes occurring along the Cenozoic, including several changes of the coastline position caused mainly by glacioeustasy [20,49,52–55].

The continental shelf has a gentle slope, and the shelf break occurs at a water depth between 160 and 200 m [20,24,56]. The inner continental shelf is characterized by an elongated SW–NE seafloor depression, which represents the RdIP paleovalley [22,24,53,54,57,58]. This depression was about 35 km wide and up to 50 m deep before it became partly filled by sediments [24]. Its present-day seafloor physiography is described by [53,54,57,59]. South of this paleovalley, the inner shelf shows a complex of relict barrier islands and sandbanks that constituted the major morphosedimentary features developed in the region during the post-glacial transgression [53,54,57,60,61].

Whereas the outer- to mid-shelf displays a relatively rough surface, the outermost shelf is characterized by a terrace-like shape and a smooth relief. The rough surface is

interpreted as the product of differential exposure of sediments during regressions and transgressions of the Quaternary [24].

On the continental slope, a well-developed contourite depositional system (CDS) exhibits both erosive (terraces and channels) and depositional (drifts) features associated with the action of different Antarctic water masses and their interfaces [23,62]. Thus, these features are well developed along the Argentinean margin and gradually disappear towards the north, where across-slope (turbiditic) processes dominate [61,63]. Submarine canyons systems (SCS) were first reported by [64], between 35° and 38° S, and recently described by [23,65,66]. Several canyons dissect the continental slope off northern Argentina and Uruguay. Some of these canyons cut back into the shelf break but do not show major incisions on the shelf itself [23,64].

2.3. Sedimentological Characterization

The sediment distribution is closely associated with the regional circulation. Relict sand cover dominates the shelf and was deposited under the littoral barrier and estuarine environments, which were reworked during several Plio–Pleistocene transgressive–regressive events [53,54]. Sediments of Pampean–Patagonian origin distribute along the Argentinean margin to the RdIP mouth and are transported northward by the MC [67,68]. Several authors concur regarding the influence of pyroclastic and volcanic sediments of Pampean–Patagonian origin transported northwards by the MC [67,69–71].

The continental slope is influenced by a combination of modern transverse, longitudinal, and vertical processes. Modern mass gravity processes in the middle and lower slope [72,73] are associated with seismic movements in the fracture zone [73,74]. Due to their small-scale nature, they do not represent a significantly associated geohazard. Modern transversal transport of sediments occurs from the shelf to the upper slope [65,75], probably associated with the STSF as well as related to submarine canyons heads [65,66]. Small-scale gravitational processes promote the lateral flow of organic matter (Hensen et al., 2000) from the Argentinean shelf towards the lower slope. On the lower slope, and off the RdIP, sedimentation of terrigenous particles results from RdIP discharge [76]. As a result, a hemipelagic sedimentation model for the RdIP sediments associated with the Brazil–Malvinas Confluence was proposed [65,76].

A large part of the continental discharge of the RdIP is deposited in the river's mouth and towards the northeast along white clay–silt facies (“mud belts”) on the inner continental shelf [20,22,77] and towards the Brazilian shelf [68,78]. This facies corresponds to the RdIP paleovalley [79,80]. Within the “mud belts” [39,80,81] a proximal zone is differentiated in which current deposition of suspended sediments of the RdIP occurs from a distal zone characterized by relict sediment. These authors point out the influence of the STSF as a barrier to the present sedimentation of RdIP particles. However, studies on the Brazilian continental margin [82,83] suggest the influence of organic matter originating from the RdIP on the Brazilian continental shelf. Sandy sediments from the Uruguayan basement are distributed south of the RdIP paleovalley [53,54].

2.4. Oceanic Carbon Cycle

Through primary productivity (PP)—the uptake of dissolved inorganic carbon (DIC) and its sequestration into organic compounds by marine primary producers—but also via CaCO₃ (carbonate) formation by biomineralizing biota, oceans act as regulators of the carbon biochemical cycle, which affects the balance between the ocean and the atmosphere. The distribution of carbon in the ocean is linked to biological productivity, sinking and degradation of organic matter and calcium carbonate, and ocean circulation [84]. Benthic foraminifera respond to pulses in the organic particle flux by increasing their biomass [85,86] at a fast rate, while bivalves and other benthic suspension and deposit feeders may show the slowest responses [87]. A quantitative relationship between the benthic foraminiferal density and ocean surface productivity has been recognized, constituting one of the best trophic proxies for the organic carbon flux (J_z : PP superficial percentage that reaches the bot-

tom, taking into account the consumption processes, but not the lateral advection processes) to the seafloor [83,85,86,88–91]. The trophic state and other environmental conditions (e.g., energy and nutrient contents) are reflected in benthic foraminifera and other assemblages (e.g., density, specific composition, diversity, and vertical distribution [77,83,92–95]).

In the UCM, the input of organic carbon from local autochthonous processes over the outer shelf, break, and the slope is presumed to be quantitatively important in near-surface and subsurface layers. However, direct estimates of surface primary production rates are critically scarce and limited to the mid-outer shelf (few estimates near the 100-m isobath, [96]) and available estimates for the slope or deeper waters are lacking. Indirect estimates derived from satellite data (MODIS-Aqua) and modeling exercises based on mean-field photosynthetic parameters for this specific oceanic province indicate high productivity with values similar to upwelling regions (e.g., Cabo Frio, Brazil [83]) on the outer Argentinian shelf and break immediately south of the RdIP, and on the southern portion of the Uruguayan margin (values ranging between $365 \text{ gCm}^{-2} \text{ year}^{-1}$ and $1362 \text{ gCm}^{-2} \text{ year}^{-1}$ [95,97]). This occurs particularly during summer and to a lower extent in spring. Further, according to [98], satellite-derived productivity data on the UCM could be confounded by elevated amounts of dissolved organic matter in the RPP and should be taken cautiously [98].

Estimated values of J_z between $26 \text{ gCm}^{-2} \text{ year}^{-1}$ and $442 \text{ gCm}^{-2} \text{ year}^{-1}$ are negatively related to water depth indicating consumption, degradation, and lateral transport by bottom currents [95]. The southern portion of the UCM shows higher values than the northern portion to PP, J_z , exhibiting benthic foraminifera species (specially opportunist and infaunal species) typical of high productivity regions (e.g., *Epistominella exigua*, *Bulimina* spp, *Globocassidulina* sp., *Uvigerina* spp., *Fursenkoina* sp. *Nonionella* spp., *Reophax* sp.) and Benthic Foraminifera High Productivity index (BFHP) [95,99,100]. High productivity is likely favored by fresh nutrients carried by the Malvinas Current [95]. Further support is evidenced by the distribution of scallop beds occurring on the Patagonian shelf, referred to as being controlled by low availability of food in the northern portion of UCM, thus setting its northernmost distribution limit [101].

Elevated phytoplankton concentrations have been reported associated with frontal structures in the BMC zone [102–104]. Reference [76] describes the presence of a north–south direction corridor (between 52° and 54° W) with high C_{org} values ($>2.5\%$) between 500 and 3500 m depth. According to the authors, this corridor is the product of high PP in the surface due to of the encounter of the MC and BC the RdIP contribution. Although all proxies of organic matter origin ($\delta^{13}\text{C}$, $\delta^{15}\text{N}$, Ba/Al, Ba/Ti, and C/N) indicate the marine origin and labile quality [105,106], some values related to the southern portion of the UCM and related to the corridor described by [76] could indicate organic matter of continental origin and more refractory quality matter.

Biomass or phytoplankton abundance may not be accurate indicators of productivity, though, since, at any given point in time, they represent a balance between gain (production) and loss (i.e., grazing) terms. These processes are strongly dependent on the structure of the phytoplankton community and physical dynamics [107,108], and over the Uruguayan shelf, significant decoupling between production and biomass was reported and attributed to the variability in referred loss rates (i.e., grazing [96]). C_{org} values reported for the sediment show that these do not always follow the expected pattern according to the distribution of PP and J_z [95]. This indicates consumption and degradation during the sedimentation process (along the water column) and energy processes (lateral and offshore transport).

Following the bathymetric gradient, from 3000 m (lower slope) offshore, a strong decrease in C_{org} , organic matter, and N_t concentration, as well as foraminifera density, is registered [99,100]. In deep waters J_z that reaches the sea bottom depends on the PP and remineralization of the organic matter along the water column. In this sense, the labile organic material (metabolizable) decreases with depth. This is reflected in the decreasing density of the benthic foraminifera and a shift in their feeding strategies, dominated by detritivorous species (e.g., *Stainforthia complanata*, *Uvigerina peregrina*, *Cassidulina* spp. [99]).

In agreement, most mollusc bivalves reported from the deep sea are deposit feeders and carnivore species (*Septibranchia*) [109].

Time variability of chlorophyll-a from satellite data can provide insights into spatial patterns in production. Following this rationale, significant effects were detected at seasonal and interannual time scales linked to ENSO variability in the outer shelf and slope off Uruguay [110]. Higher biomass (and presumably production) during El Niño years seem to result from enhanced flow and nutrients delivery by the RPP, and its advection by surface wind anomalies under El Niño conditions [43].

Canyons are typically associated with increases in local primary productivity with consequences for the entire food web. Satellite images clearly show these increases in the UCM associated with these structures and are probably related to the upwelling of the SAW and AAIW (rich in nutrients) that reaches the surface contributing to the observed high productivity [95]. High percentages of C_{org} (>2.06%) and high densities of infaunal benthic foraminifera belonging to hyaline genera, detritivorous feeding, and indicators of dysoxic conditions (*Bolivina* spp, *Bulimina* spp, *Fursenkoina pontoni*, *Nonionella* spp, *Uvigerina* spp [95,99]) are present in these areas. High percentages of refractory organic matter area are also present in these environments.

The shallowest zone (inner shelf) receives a significant contribution of nutrients from the RdIP and is characterized by high chlorophyll values (ca. $8 \mu\text{g L}^{-1}$) associated with the RPP [22]. Similar values (ca. $6.5 \mu\text{g L}^{-1}$) could be observed in the RdIP immediately offshore of the turbidity front [77]. Additionally, high chlorophyll values (ca. $5.5 \mu\text{g L}^{-1}$) characterize the local upwelling at the edge of the paleovalley [22]. In this case, the edge of the paleovalley is represented by an ancient coastline (dominated by coarse sediment) and characterized by low C_{org} values (0 and 0.26%). Nevertheless, marine productivity proxies (Si/Ti, Ba/Ti, Ca/Ti, and P/T) indicate high productivity with values higher than those reported from the RdIP [77] and the outer shelf and upper and middle Uruguayan slope [105]. Benthic foraminifera show high diversity, including infaunal and epifaunal species with herbivorous and detritivorous feeding strategies (e.g., *Quinqueloculina milletti*, *Quinqueloculina atlantica*, *Elphidium williamsoni*, *Textularia earlandy*, *Brizalina striatula*). This reflects a local wealth of food availability, while the different microhabitats reflect the complex geomorphology of the environment (ancient coast with mollusk fragments) [111].

The paleovalley sediment is characterized by high C_{org} concentration (values between 0.5 and 1.2%). These values are similar to those registered by [77] in the RdIP, especially in sediments affected by the turbidity front. Fine-grained mineral and organic particles are characterized by a similar settling mechanism [112]. The foraminifera fauna is represented by detritivorous infaunal species, followed by herbivorous infaunal forms (*Buliminella elegantissima*, *Nonionella atlantica*, *Ammonia tepida*, *Hoeglundina elegans*), indicating organic enrichment, low energy and oxygen conditions [111].

There is a clear spatial gradient in terrestrial influence, decreasing from the RdIP to the inner shelf off Punta del Este, confirmed by stable carbon and nitrogen isotope values ($\delta^{13}\text{C}$ and $\delta^{15}\text{N}$) as well as C/N ratio [22]. However, there are no available values for these proxies from nearshore areas ($\delta^{13}\text{C}$ and $\delta^{15}\text{N}$), nor C_{org} concentration estimations, since the sediment is composed of coarser sands reflecting the predominant high energy precluding local deposition. Nevertheless, other marine productivity proxies (Si/Ti, Ba/Ti, Ca/Ti, and P/Ti) indicate low productivity in the local area [22]. Benthic foraminifera fauna from this area also suggest a high energy environment (e.g., *Quinqueloculina atlantica*, *Quinqueloculina milletti*, *Textularia earlandy*, *Elphidium discoidale* [111]). On the other hand, there is a clear increasing gradient of C_{org} concentration in the sediment, from the inner shelf to the outer shelf and the break. The foraminifera fauna also shows a clear density increase associated with this gradient [99,100].

3. Development and Structure of Conceptual Models

The choice of format was based on the analysis of the environmental context presented above. Tectonic, climatological/hydrodynamical, and geomorphological processes and

structures were identified as the main natural drivers of the UCM (see Figure 4) and were included in the models. Geomorphology was used as the common “base layer” in the conceptual models (Figure 2) because it is considered an objective and fixed spatial reference frame in a large temporal scale range.

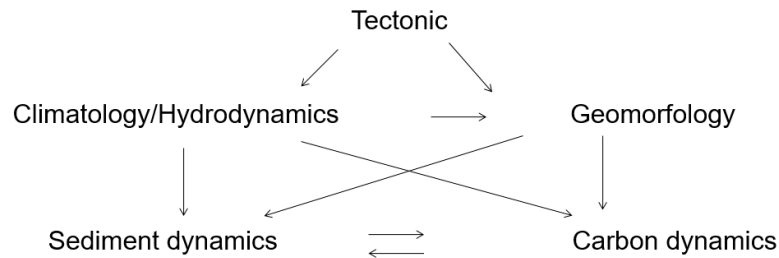


Figure 4. Schematic representation of the interrelation of physical drivers and oceanographic processes represented in the models.

Development of the model structure was determined to simplify the UCM system into less-complex systems (see Figure 5).

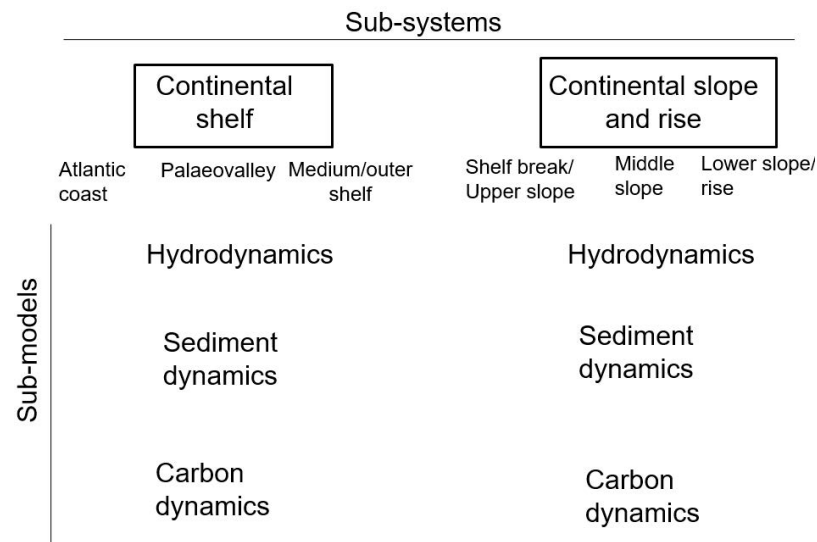


Figure 5. Schematic representation of the structure of conceptual models. Each sub-system (continental shelf and continental slope/rise) is described by three sub-models (hydrodynamics, sediment dynamics, and carbon dynamics). Different sedimentary environments (i.e., Atlantic coast) further characterized each sub-system.

On the horizontal axis, system decomposition consists of separating a more extensive area into habitats. The horizontal subdivision (subsystems) was determined mainly by their general geomorphological and hydrodynamical characteristics, determined by a combination of environmental factors acting on a geological scale. It includes two geographical areas; (a) continental shelf (from the Atlantic coastline to 180 m depth); and (b) continental slope and rise (between 180 and 4500 m depth; Figure 2). These subsystems were further divided based on distinct sedimentary environments (see Figure 5). These ecosystems are interconnected, and interaction between them is presented in the models as external links. The exposed Atlantic littoral zone and the RdIP estuary, that connect the continent with the oceanic environment, are very complex systems, and have been studied by many authors (previous works were carried out within the framework of the projects [113] and <https://www.gub.uy/ministerio-ambiente/politicas-y-gestion/programa-ecoplata>, accessed on 7 December 2020; also see [114–116]. Consequently, they would require the

development of specific models that exceed the objective of this work. However, the influence of these environments on the study area is considered in the models.

For each subsystem, three sub-models were developed, namely hydrodynamics, sediment, and carbon dynamics. The information included in each sub-model is ordered according to different attributes (i.e., processes; see definition below). Each sub-model is represented by a 3D diagram superimposed on the “geomorphological base layers” including flowcharts of the main processes, and is accompanied by texts that succinctly describe the processes represented in the schemas. The processes described in the text correspond numerically to the processes represented in each 3D diagram, and together they depict the dynamics of each subsystem. The sources of text information are cited accordingly, and hypothesized processes and linkages are named “expert judgment”. The elaboration of these models implies integrating, organizing, and synthesizing current knowledge about UCM dynamics, identifying information gaps, and documenting assumptions about processes and the interaction between these processes and the environmental dynamics. Accordingly, this work aims to provide a comprehensive framework based not only on the current knowledge; but also on working hypotheses that arise from expert judgment.

Hydrodynamics. These sub-models describe processes related to the movement of fresh, coastal, and oceanic waters and variations in temperature and salinity. They include the input of continental water, oceanic circulation (water masses, currents, fronts, wind waves), stratification/vertical mixing processes, and the relative energy of the environment.

Sediment dynamics. These sub-models describe sources and transport routes as well as depositional characteristics of fine and coarse sediments. They include the entrance of fine (silts and clay) and coarse (sand and gravel) sediments, as well as transport, erosion/deposition, exposure, burial, and resuspension processes.

Carbon dynamics. These sub-models describe biogeochemical processes intimately linked to organic carbon fluxes, emphasizing the entrance and cycling of marine and terrestrial particulate material, biological production, carbon flux (J_z), and deposition of organic carbon. We also look at DIC fluxes (i.e., photosynthesis and CaCO_3 formation) to organic and biomineralized carbon. Due to the complexity of the biological trophic web and ecological processes, we only focused on critical biological components (i.e., surface primary producers, benthic heterotrophic foraminifera, bivalves, and deep-water corals) that provide valuable information regarding the link between the physical and biological compartments.

4. Conceptual Models of the UCM

4.1. Subsystem 1: Continental Shelf (0–180 m)

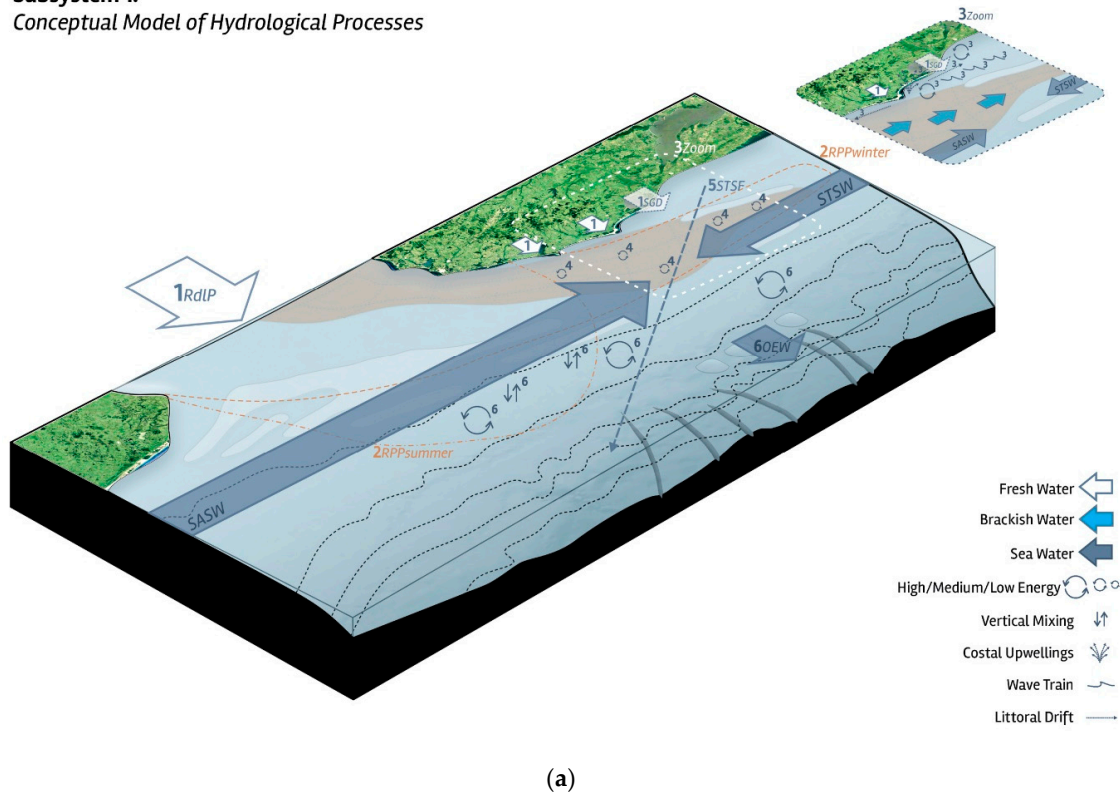
This subsystem includes the Territorial Sea and part of the Uruguayan EEZ (Figures 1A and 2) from the coast to 180 m depth. From the geomorphological point of view, this region covers the continental shelf, constituted by diverse sedimentary environments defined according to their location from the coast to the offshore and following [53] (Figure 2).

These environments are (I) “Atlantic coastal sands” (i.e., from the low-water mark to the RdIP paleovalley) which include relicts of ancient shorelines, chimneys, and oil seeps; (II) the “RdIP paleovalley” distributed at approximately 40 km from the coast and the shallow marine zone; and (III) “Relict sands” (i.e., offshore of the RdIP paleovalley, i.e., from the inner and middle shelf to the shelf break. This region includes relicts of ancient shorelines, chimneys, and oil seeps. The hydrodynamic scenario is governed by the Río de la Plata Estuary (RPE), RPP, and STSF.

4.1.1. A Conceptual Model of Hydrodynamics Processes: 3D Diagram and a Brief Description of Processes

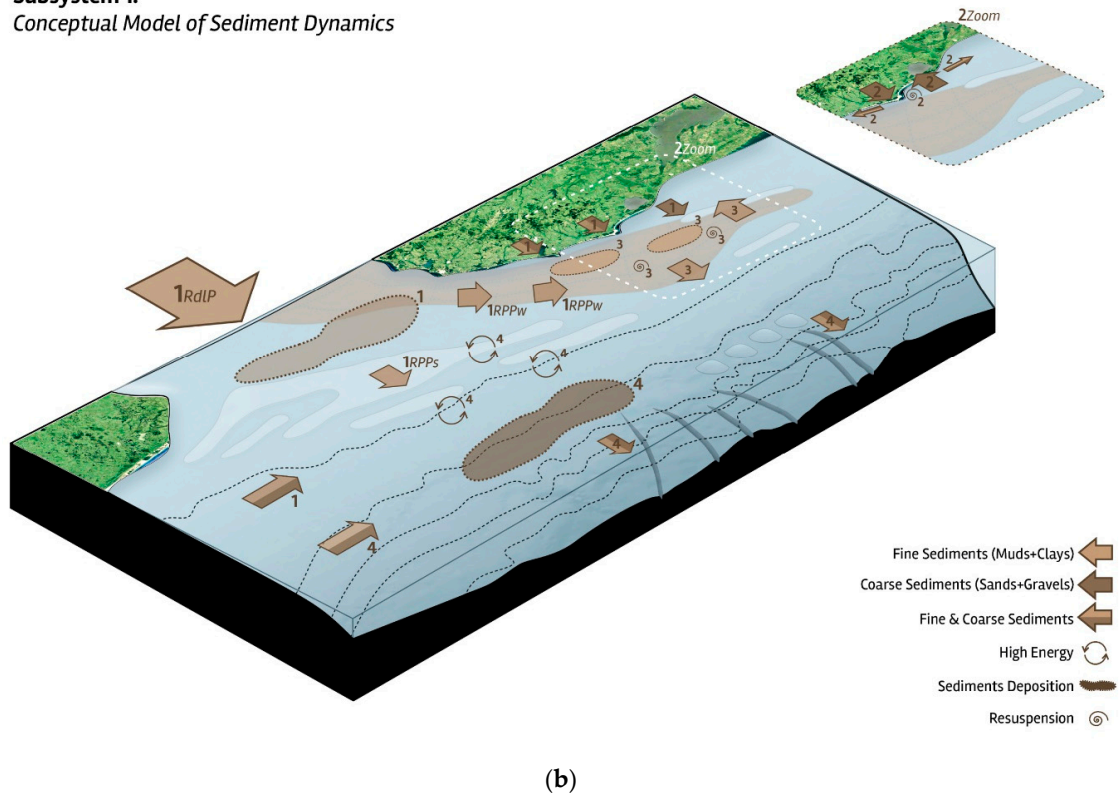
Figure 6a shows the model of hydrodynamics process in the Subsystem 1.

Subsystem 1:
Conceptual Model of Hydrological Processes



(a)

Subsystem 1:
Conceptual Model of Sediment Dynamics

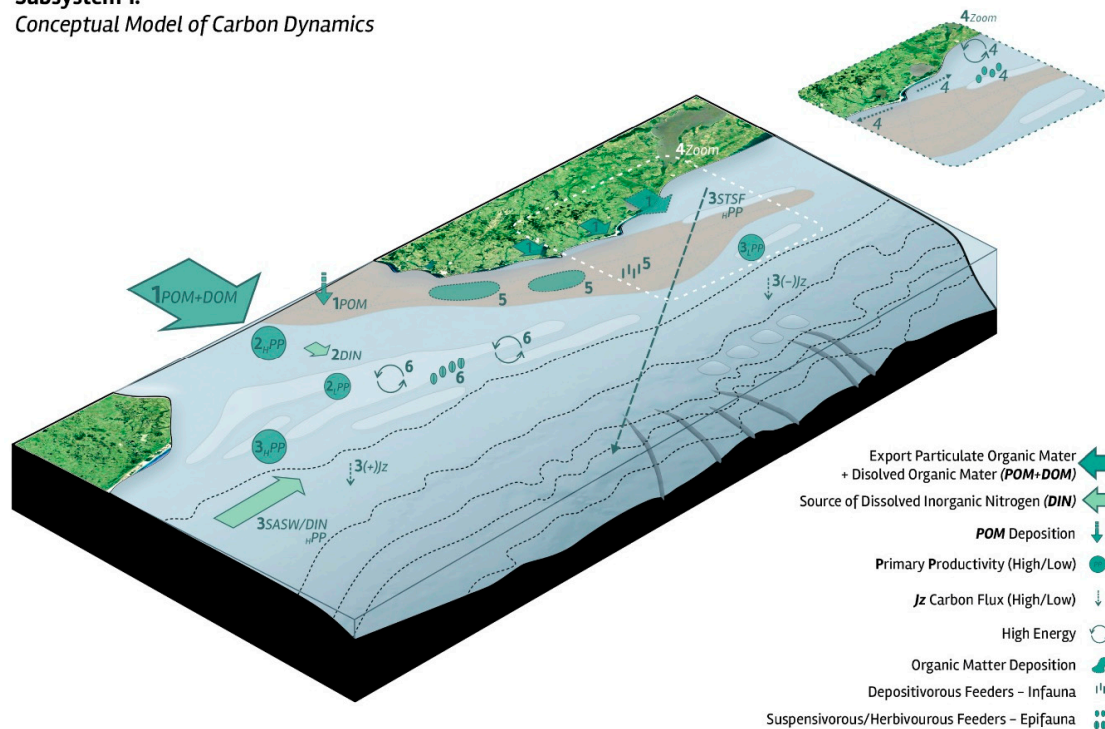


(b)

Figure 6. Cont.

Subsystem 1:

Conceptual Model of Carbon Dynamics



(c)

Figure 6. (a): Conceptual hydrodynamical process model (subsystem 1; continental shelf 0–180 m). Subantarctic Shelf Water (SASW), Subtropical Shelf Water (STSW), Subtropical Shelf Front (STSF), Río de la Plata (RdIP), Río de la Plata Plume (RPP), submarine groundwater discharge (SGD), oceanic exportation water (OEW). (b): Conceptual model of sediment dynamics (subsystem 1; continental shelf 0–180 m). Río de la Plata (RdIP), Río de la Plata Plume suspended sediment (RPPs), Río de la Plata Plume water (RPPw). (c): Conceptual model of carbon dynamics (subsystem 1; continental shelf 0–180 m). Subantarctic Shelf Water (SASW), Subtropical Shelf Front (STSW).

1. An immense contribution of continental water occurs through the RdIP discharge; $24,000 \text{ m}^3/\text{s}$ [117,118] with maximum flow in March–June and September–October and minimum in summer [119,120]. On a smaller scale, there is also continental contribution through minor estuaries (Arroyo Maldonado, Pando, Solis Chico, and Grande) and some lagoons sporadically connected with the ocean (Lagoon of Castillos, Rocha, Garzón, and José Ignacio [121]). The total continental discharge varies according to the intra- and interannual climatic conditions, mainly related to ENSO, and is directly associated with rains occurring in the RdIP basin and local storms. This flux is also under growing anthropogenic influence, related to the land-use change (urbanization, agriculture), and the consequent modifications in run-off due to alteration of the hydrological cycle [122,123]. Submarine groundwater discharge (SGD) is another mechanism expected to contribute significant amounts of fresh water, nutrients, and other elements (Fe, Mn) to the inner continental shelf, as reported for the Southern Brazil region and elsewhere [124–126].

2. The RPP is characterized by high turbidity ($<1\text{--}78 \text{ NTU}$) and low salinity ($<1\text{--}32$) [97,127], displaying a steep gradient from the river mouth to the outer shelf and Atlantic coastal region, especially between Montevideo and Punta del Este. The flow of the RPP is driven by Coriolis and seasonally variable winds. In winter, it moves towards the NE and NE–E parallel to the coast covering the coastal zone and the paleovalley (related with a higher frequency of southern winds). In summer, it moves to the outer shelf in front of the mouth of the RdIP and continental slope (related with a higher frequency of northern and eastern winds). Under high rainfall and river discharge conditions, such as during ENSO warm phase [18,42,95], winds and the RPP follow the summer pattern conditions.

The influence of the RPP promotes water column stratification and the development of a saline front [17,18,22,128]. The seawater under the plume is mainly Subantarctic Shelf Water (SASW), although Subtropical Shelf Water (STSW) also enters during summer. In some conditions, a mixture of both masses can be observed [18,22,129].

3. The interaction of shelf waters with the seabed and with the coastline is reflected in wave action, tides, littoral drift (lateral transport), and coastal upwellings. This is particularly strong during extreme storm surges, causing the sea-level rise [116,130–132]. South of the rocky promontory of Cabo Polonio (Rocha) the littoral drift flows southward (SW, W) while to the north of this promontory, it moves eastward (NE) [116,123,133]. In turn, from Cabo Polonio to the NE, the resulting sediment volumes transported by littoral drift are highly significant, while for the Atlantic and estuarial coast it has been estimated at around tens of thousands m^3/year [133]. However, estimations for the neighboring Chuy-Lagoa Mangueira section (Brazil) suggest a sediment volume in the order of 2,747,000 m^3/year [116,134]. The action of NE and E swells and the orientation of the coastline promote the offshore displacement of coastal surface waters and the upwelling of shelf bottom water mainly in summer conditions [22,135–137].

4. The paleovalley presumably acts as a natural barrier against the displacement of shelf currents [24], promoting a low-energy environment and the concentration of the RPP [22]. Additionally, as a deeper channel, the paleovalley allows the drainage of riverine waters at the surface and the entry of seawater at the bottom, enhancing stratification due to differences in density, mainly governed by salinity [22,138].

5. Offshore of the paleovalley, the RPP causes stratification of the surface water column. The STSF dominates the sub-superficial levels (below the RPP). The STSF results from the convergence of the Subtropical Shelf Waters (STSW, flowing southward) and Subantarctic Shelf Waters (SASW, flowing northward [18]). This front shows a relatively seasonally stable distribution [42]. In the STSF, there is little or no mixing between STSW and SASW [18]; however, it does not impede the circulation of marine plankton [139].

6. The relatively high intensity of shelf currents causes vertical mixing and the dominant high energy conditions on the benthic environment [99,100]. This energetic environment is further intensified in the vicinity of relicts of ancient shorelines [99,100,140,141]. Upon reaching the STSF, a large part of STSW is likely exported offshore, where the SASW is less energetic than STSW [142].

4.1.2. A Conceptual Model of Sediment Dynamics: 3D Diagram and a Brief Description of Processes

Figure 6b shows the model of sediment dynamics in the Subsystem 1.

1. The RdIP carries around 160×10^6 metric tons per year of suspended sediment to the Atlantic [143]. Most of the fine sediment transported by the RdIP is retained in the estuary and flocculates on the estuarine front [144]. The non-retained sediment penetrates on the shelf suspended in the RPP [145]. This flow represents the main route of entry of fine sediments into the SW Atlantic shelf. On a smaller scale, fine sediments also enter through the discharge of minor Atlantic estuaries [121], and are suspended in the water column, from the Argentinean continent, and through the shelf [146]. Coarse sediments arrive at the shelf transported from the south (Argentina) by the SASW [24] and also (although presumably several orders of magnitude below) by erosion of the exposed Atlantic coastal zone by processes associated with sea-level rise [53,123,130,131,147].

2. The high energy associated with waves and storms dynamics likely inhibits fine sediments deposition and promotes the exchange of coarse sediments between the raised and the submersed coastal zone [123]. There is an alternation between erosion, exposure, and the burial of sediments in the submerged zone [53,123]. Transport of sediments also occurs along the Atlantic coast, associated with coastal drift [116,123].

3. Much of the fine sediments that reach the shelf, transported by the RPP, are deposited in the paleovalley. Its sedimentation shows values of $8 \text{ mm}/\text{year}^{-1}$ and a gradational stratification pattern [24,148]. Nevertheless, resuspension of the fine sediments

previously deposited in the paleovalley can presumably occur, with a consequent transport to the offshore (expert judgment).

4. Offshore of the paleovalley, the dominant high energy avoids the permanent sedimentation of fine sediments (expert judgment). The shelf currents erode, rework, and expose relicts of ancient shorelines [22,24,53]. Coarse sediments transported from the south are deposited on the outer shelf, south of the STSF [24], probably associated with the relatively lower current energy-carrying STSW (expert judgment). Sediment transport from the shelf and towards the slope related to the STSF circulation is reported [65,75,149,150].

4.1.3. A Conceptual Model of Carbon Dynamics: 3D Diagram and a Brief Description of Processes

Figure 6c shows the model of carbon dynamics in the Subsystem 1.

1. Most of the continental particulate material transported by the RdIP is deposited near the estuarine front due to a combination of hydrodynamical and biogeochemical processes [77,122,127,151]. The presumed non-retained continental material enters through the shelf along with the RPP. Dissolved organic matter (DOM) originated in the RdIP presumably constitutes the mayor input of the ocean (expert judgment). To a lesser extent, materials also enter via smaller estuaries or sub-estuaries within the RdIP [122,123,152–154]. Nutrients and organic matter may also reach the area via submarine water discharge [124,155]. The RPP and water masses (e.g., SASW, STSW) dynamics favor lateral advective transport towards the Uruguayan shelf [19].

2 The RdIP itself is a highly productive area. Most dissolved inorganic nitrogen (DIN; limiting nutrient in the RdIP estuary and RPP waters) [127,151,153,156] from continental runoff is assimilated within the RdIP estuary. Maximum primary production within the RdIP occurs in the mesohaline region seaward of the turbidity front, ca. 100 km from the estuary–shelf transition [127]. At the transition between the estuary and the inner shelf (water column depths between 20 and 50 m), the RPP carries very low amounts of DIN while primary production and phytoplankton biomass decrease sharply [96,127]. Most particulate matter produced within the RdIP is thus either consumed or deposited within the estuarine basin. Part of this particulate organic carbon (POC) is consumed in the benthic environment, e.g., by the clam *Mactra isabelleana*. This facultative deposit feeder occurs all along the turbidity front, incorporating both dissolved inorganic carbon (DIC) into shells and dissolved organic carbon (DOC)/(POC) into biomass. During the warm ENSO phase (El Niño periods) the strongly increased freshwater runoff would move the estuarine frontal system further offshore, favoring the fertilization of the shelf area [41,157].

3. Local neritic primary production over the shelf is driven by the interplay of dominant water masses: STSW, SASW, and RPP [97]. Between ca. 100–200 m, SASW constitutes the main source of DIN [156,158], higher primary production was observed associated with thermal fronts and, where SASW is present, also within the euphotic zone [96]. Also, PP (according to MODIS-Aqua data), J_z and foraminiferal species indicators of high productivity are higher on the southern portion of the Uruguayan margin than on the northern sector [95,97,99,100]. This occurs particularly during summer (and to a lower extent in spring) and is likely favored by the Malvinas Current presence, rich in nutrients [95]. This is reinforced by the presence of the planktonic foraminifera species (*Neogloboquadrina pachyderma* and *Neogloboquadrina incompta*) transported by the ASA [99,100]. According to benthic foraminifera data and geochemical indicators, there is a positive gradient in PP from the inner shelf to the outer shelf [99].

4. In the inner shelf and coastal areas, the high dominant energy promotes the mixing of the organic material, enabling organic deposition [99,100,111] and presumably promoting lateral transport and resuspension, as well as the dominance of benthic epifaunal foraminifera, suspensivorous/herbivorous feeders, indicators of high dynamics conditions, as well as well-oxygenated habitats (e.g., Miliolida [99,100,111]).

5. Much of the organic material associated with the RPP (refractory organic matter [77]) is deposited in the low energy zone of the paleovalley controlled by the same factors as fine lithogenic material [22,148]. In agreement with this, deposition and burial of

organic matter and dominance of benthic infaunal foraminifera depositivores (e.g., Buliminidae) and bivalves (e.g., Nuculinidae, deposit feeders that can supplement their diet with limited suspension-feeding and live infaunal, buried in sand or mud sediments with high organic matter content) occur in this area [111,159,160]. This organic material and fine sediment may also undergo deposition and r-suspension aided by biological activity such as burrowing [111]. PP and organic matter depositions are enhanced by the presence of a local upwelling related to an ancient coast that acts as the edge of the paleovalley [22].

6. Relict ancient shorelines are structures under energetic hydrodynamical conditions, and consequently, the organic matter produced on the surface is not deposited in the seabed. Robust tests of epifaunal herbivorous and suspensivorous foraminiferal species (especially Miliolida) are associated with these environments [99,111].

4.2. Subsystem 2—Slope/Continental Rise (180–4500 m)

This subsystem includes part of the Uruguayan EEZ (Figures 1A and 2) and covers from 180 m deep to 4500 m deep. From the geomorphological point of view, it represents the continental slope and the continental rise, characterized by the CDS mainly south of the area and a progradational margin (PM) in the north, and diverse sedimentary environments constitute it. These environments are defined according to their location from the shelf break to the offshore (Figure 2) and are named as follows: (IV) shelf break and upper slope (i.e., 180–500 m deep); (V) middle slope (i.e., between 500 and 1500 m deep), and (VI) lower slope/continental rise (1500–4500 m deep). Distinct morphologies include contouritic terraces, channels and drifts, submarine canyons, seamounts, chimneys, and oil seeps. The hydrodynamic/oceanographic scenario is governed by the BMC (Figure 1B).

4.2.1. A Conceptual Model of the Hydrodynamics Processes: 3D Diagram and a Brief Description of Processes

Figure 7a shows the model of hydrodynamics processes in the Subsystem 2.

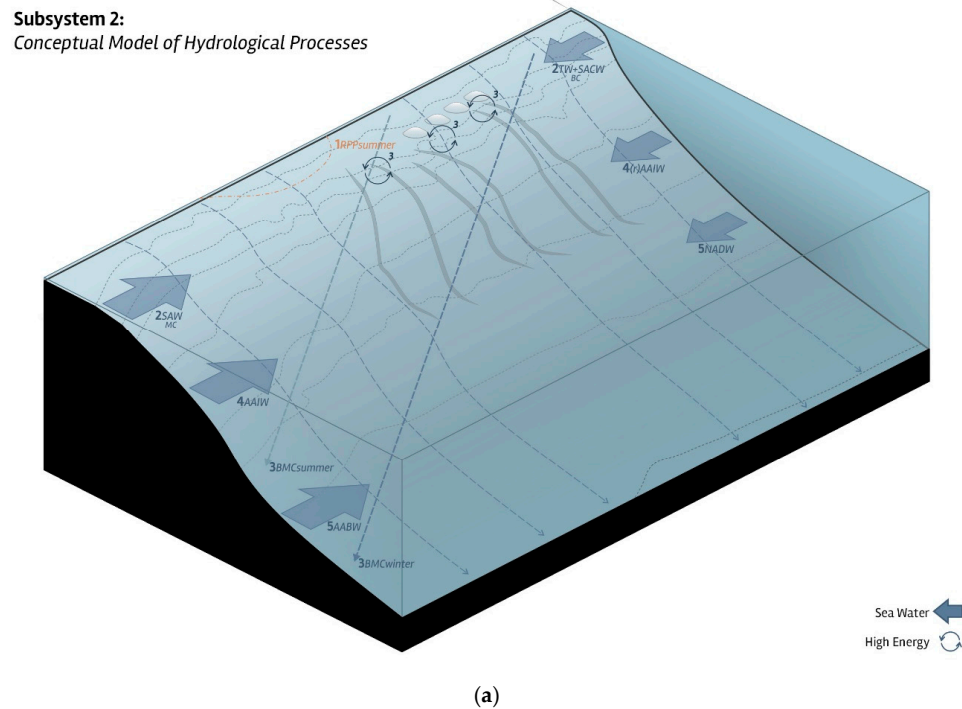
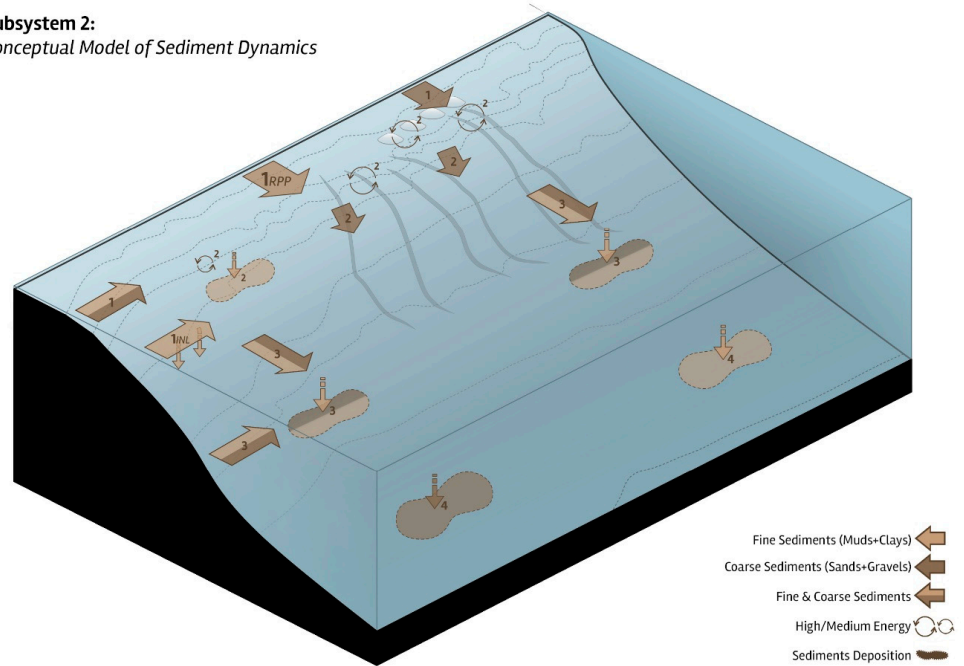


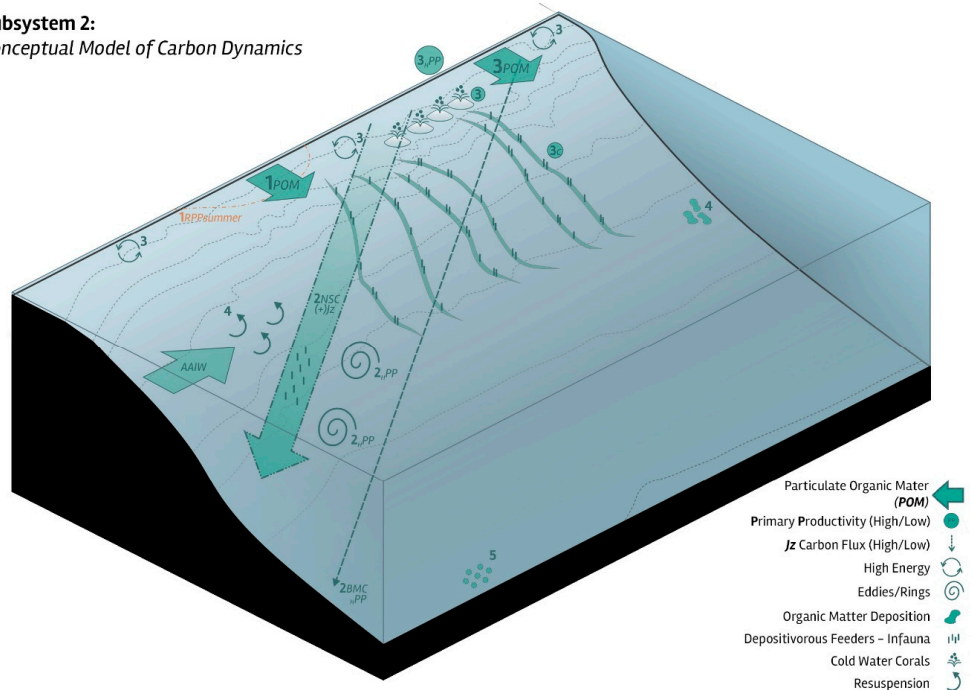
Figure 7. Cont.

Subsystem 2:
Conceptual Model of Sediment Dynamics



(b)

Subsystem 2:
Conceptual Model of Carbon Dynamics



(c)

Figure 7. (a): Conceptual model of the hydrodynamics process (subsystem 2; slope/continental rise 180–4500 m). Río de la Plata Plume (RPP), Subantarctic Waters (SAW), Tropical Water (TW), South Atlantic Central Water (SACW), Antarctic Intermediate Water (AAIW), recirculated Antarctic Intermediate Water (AAIW_r), Malvinas Current (MC), Brazil Current (BC), Brazil–Malvinas Confluence (BMC), North Atlantic Deep Water (NADW), Antarctic Bottom Water (AABW). (b): Conceptual model of sediment dynamics (subsystem 2; slope/continental rise 180–4500 m). Río de la Plata Plume (RPP), intermediate nepheloids layers (INL). (c): Conceptual model of carbon dynamics (subsystem 2; slope/continental rise 180–4500 m). Río de la Plata Plume (RPP), Antarctic Intermediate Water (AAIW), Brazil–Malvinas Confluence (BMC).

1. The RPP dominates surface waters (approx. 10–40 m from the surface) of the continental slope during the summer and El Niño events [18,95], promoting stratification of the water column.

2. Below the RPP (in summer) and during the winter season, the waters over the shelf break/upper slope are dominated by waters advected by the Brazil and Malvinas currents [19,25,65,161,162]. Warm subtropical waters (TW and SACW, transported southward by the BC) and cold Subantarctic Waters (SAW, transported northward by the MC) dominate the northern and southern areas, respectively. An evident seasonal variation characterizes this process; during the summer, the BC is intense, and the MC is relatively weak, leading the warm waters to influence the entire UCM. During autumn, the MC intensifies and extends up to 35° S. The migration of the BMC coupled with the atmospheric synoptic activity generates instabilities in the ocean, which causes large variations of the currents at relatively small spatial and temporal scales (in terms of days [163]). A strong thermocline occurs below the SACW at approximately 500 m deep [25].

3. The shelf break/upper slope is a highly energetic zone associated with the dynamics of the STSF and BMC and the conspicuous morphology of the shelf-break [65,149]. The energy of this environment is intensified to the north of the area controlled by the BC and by the progradational margin. It is particularly intense in the vicinity of seamounts and at the head of submarine canyons [105].

4. On the middle slope, the Antarctic Intermediate Water (AAIW) flows northward as a fresh and oxygenated water mass below the SAW, while the recirculated AAIW flows southward below the BC [164]. The interaction of the recirculated AAIW and the progradational margin promotes a region of relatively low energy at the north. To the south, the energy is higher due to fresh AAIW on a concave margin [65].

5. On the lower slope/continental rise, the North Atlantic Deep Water (NADW) flows to the south with an estimated transport of 15–20 Sv [165] below the Antarctic Bottom Water (AABW), one of the densest and most voluminous water masses of the global ocean, that plays an essential role in transporting carbon, heat, and freshwater sequestered from the atmosphere to the deep ocean [166,167] and flows to the north with the transport of 1.8–3.6 Sv [35].

4.2.2. A Conceptual Model of Sediment Dynamics: 3D Diagram and a Brief Description of Processes

Figure 7b shows the model of Sediment Dynamics in the subsystem 2.

1. The entrance of fine sediments is presumably through the RPP on the surface [76], resuspended from the Argentinean shelf [105] and from intermediate nepheloids layers (INL) related to the AAIW [168]. The input of coarse sediments occurs from the adjacent continental shelf as well as from the Argentinean slope [24,65,75,105].

2. The high energy of the shelf break/upper slope promotes erosion, being particularly intense in the north (PM) and in the vicinity of the canyons and seamounts. This promotes the transport of coarse sediments from the shelf to the slope and into the submarine canyons, as well as the development of seamounts scarps [65,105]. In the south, relatively low energy promotes high sedimentation (400 cm/ka [75]).

3. In the middle slope, north of the margin (PM) dominates transversal and vertical transport of sediments reflected in sediment deposition controlled by the BC and by the recirculated AAIW [105]. South of the margin (CM) [65], transport of sediments from the Argentinean margin, enhanced by AAIW, dominates [23]. Transversal processes are also described [106].

4. Vertical (hemipelagic) sedimentation associated with the BMC dynamics is suggested to occur in the lower slope, characterized by fine terrigenous sediments from the RPP [76]. Very fine sands where the slopes merge with the continental rise are related to turbiditic and mass transport deposits [23,99,100].

4.2.3. A Conceptual Model of Carbon Dynamics: 3D Diagram and a Brief Description of Processes

Figure 7c shows the model of Carbon Dynamics in the subsystem 2

1. Continental input of organic matter is provided by the RPP (i.e., mixed organic matter [95,105]); however, this input is presumably orders of magnitude lower than in shallow shelf waters.

2. The input of marine particulate material occurs mainly associated with primary production triggered by the STSF and BMC [41,95,103,104,169,170]. Elevated phytoplankton concentrations are associated with frontal structures in the BMC zone (eddies, filaments, rings [102,103,171]). A sea bottom corridor located between 500 and 3500 m and oriented north–south (between 52° and 54° W) with high C_{org} values (>2.5%; constituted by labile and refractory quality matter), follows the high surface PP [76]. Benthic foraminifera is characterized by species typical of high productivity conditions [99].

3. High primary productivity values are also associated with the shelf-break front and with the dynamics of the submarine canyons [95,162]. Likewise, there is a contribution of organic matter from the shelf to the slope [74]. The high energy on the shelf-break and upper slope bottom, and the head of canyons control the non-deposition of organic matter [65,95]. The entry of organic material into the seabed in pulses has been recorded and is characterized by opportunistic foraminifera species [95]. Suspended organic matter supports monospecific cold-water corals (*Lophelia pertusa*; is associated with submarine mounds [172]). These corals support a great diversity of micro- and macrobenthic fauna [56,172]. The cold water distribution in the south of the area and the relatively low-energy conditions promote organic matter sedimentation [65]. High concentrations of organic matter are deposited inside the canyons, tripling the values found in regions near these canyons (values of up to 11.74% of C_{org} [100]. Infaunal benthic detritivorous foraminifera is also present. Dysoxic conditions characterize these environments [99].

4. On the northern middle slope, although the energy of the environment promotes sedimentation, low organic matter contents are recorded [65]. This is presumably due to the presence of the thermocline, promoting remineralization on the surface and conditioning the flow to the seabed [65,105]. To the south, contour currents transporting AAIW promote resuspension and inhibit organic matter sedimentation.

5. From 3000 m depth (lower slope) to the offshore, a strong decrease of C_{org} , organic matter, and N_t concentration, as well as foraminifera density, occurs [99,100]. The J_z organic labile material (metabolizable) is extremely low, as is the density of benthic foraminifera detritivorous species.

5. Final Remarks

Here, we present a first integrated conceptual model of the UCM. Despite the conspicuous knowledge gaps concerning the information available on key processes, a general picture of the functioning of the system is emerging in this complex biophysical setting.

5.1. Contribution on a Regional and Local Scale

At a spatial macroscale, this kind of integrative approach, although primarily based on biotic elements, and intended to function as biogeographic classification systems, is evidenced in frameworks such as the Large Marine Ecosystems (LMEs) or Marine Ecoregions of the World (MEOW). Both approaches change the focus from the management of commodities targeting the sustainable use of marine renewable resources to ensure benefits from ecosystem goods and services for the future, or assist global marine conservation planning [173]. In these schemes, regions are generally defined by ecological criteria including bottom depth contours, currents and water mass structure, marine productivity, and food webs composition and dynamics. Thus, these frameworks consider and integrate linkages between hydrodynamics, sedimentology, and the marine carbon cycle. LMEs provide a flexible approach to ecosystem-based management by identifying the driving forces of ecosystem change [174]. The LMEs system focuses on productivity and oceanographic

processes at very large spatial scales (regions on the order of 200,000 km² or greater). However, LMEs are restricted to the seaward boundaries of continental shelves, while MEOW focuses on coastal and shelf waters, combining benthic and shelf pelagic (neritic) biotas, limited by the 200-m (m) isobaths.

Similarly, in the Pelagic Provinces of the World (PPOW) scheme, provinces are large areas of the epipelagic ocean defined by large-scale, spatially and temporally stable (or seasonally recurrent) oceanographic drivers. Provinces host distinct species assemblages that share a common history of coevolution. Oceanographic drivers may include major ocean gyres, equatorial upwellings, upwelling zones at basin edges, semi-enclosed pelagic basins, and large-scale transitional elements. This scheme focused on processes occurring in the upper 200 m of the water column in off-shelf pelagic waters, including, but not restricted to, all waters beyond national jurisdiction.

In this context, our functional approach comprises a study zone that includes portions of two MEOW ecoregions (Río de la Plata and Uruguay–Buenos Aires Shelf) nested in the Warm Temperate Southwestern Atlantic, the Patagonian Large Marine Ecosystem, and probably both the Subcentral Atlantic and Malvinas Current Pelagic Provinces [173–175].

At smaller spatial scales, previous studies integrating physical and ecological processes in the area were restricted to the RdIP estuary [176] or the neritic component and dynamics of fronts over the continental shelf [16]. However, there is relatively abundant literature concerning regional and biological processes and patterns for benthic [177–179], neritic, and planktonic biota over shelf areas in the UCM, and also a plethora of very local or taxonomical restricted information that should be further explored, synthesized, and coupled with the conceptual models here presented.

Our models target an intermediate spatial scale (mesoscale), considering integrated processes occurring in the RdIP estuary, the continental shelf, and the pelagic and benthic realms over the open oceans, providing an integrative framework linking the main biophysical processes occurring in the UCM.

5.2. General Identified Knowledge Gaps

We intend that the conceptual models here presented be used as a baseline for developing quantitative models on an integrative approach. This implies developing empirical estimations of the magnitudes and rates of the processes here addressed. These include oceanographic situations promoting spatial and temporal patrons of primary production, its relationship with the community structure of phytoplankton and organic carbon exportation mechanisms and oceanic currents, and its influence on the pelagic–benthic link.

Modeling and quantifying the contribution from coastal habitats to the carbon cycle (especially by the Río de la Plata), is a significant challenge. The contribution of coastal habitats to the marine carbon cycle, including spatial/temporal influence of submarine groundwater discharge, composition, and its effects on biogeochemical cycles, need to be understood.

The relative intensity of the energy at the seabed presented in the hydrodynamics models is presumed from processes mainly associated with the granulometry distribution on the sea bottom. Thus, studies associating current energy values and grain size (see: [180–182]) are necessary to verify this assumption. In this sense, identifying, classifying, and describing the water masses, their interaction near the seabed, the speeds of the associated currents, and the distribution of sediments in the MCU region, considering depths from the outer shelf continental rise, are essential. Transport equations settings of sediment [180] and inference of sediment transport directions through the granulometric tendencies [181–183] as well as classification of geofoms as a function of velocity current flow and grain diameter in deep systems [184], will contribute to the better understanding of the processes and dynamics acting in the MCU.

5.3. Implication for UCM Management

The models will facilitate the identification of key links between drivers, stressors, and system responses. Thus, they could contribute to formulating future stressor models and monitoring plans to protect and sustain the marine environment (prevention, mitigation, and impact control).

Understanding the direct effects of climate variability and change on ecosystems and indirect effects on human activities is essential for adaptive planning to be useful in the long-term management of the marine environment.

For the UCM management, the science–policy interface could be carried out in cooperation between scientific institutions on the one hand, and government agencies on the other in a cross-border context. This policy framework is guaranteed in the attributes assigned by the Rio de la Plata and its Maritime Front Treaty through a Binational Technical Commission operating within the Ministries of Foreign Affairs of Argentina and Uruguay. The Treaty assigns the following function to the Commission: (a) fix catch volumes by commercial species and distribute them to the Parties, as well as adjust them periodically; (b) promote the joint conduct of scientific research, with special reference to the evaluation, conservation, and preservation of the living resources and their rational exploitation, and the prevention and elimination of pollution and other noxious effects that could result from the use, exploration, and exploitation of the marine environment; (c) make recommendations and submit plans tending to assure the maintenance of the value and equilibrium of the ecological systems; (d) establish standards and measures related to the rational exploitation of the species and the prevention and elimination of pollution, and prepare plans to be submitted for the consideration of the respective Governments. Although the Treaty is a key piece in area governance, the seafloor and sub-surface layers are delimited and subject to each country's jurisdiction, so challenges also exist for extending capacity and willingness to resource users.

In this scenario, and despite the uncertainties associated with quantitative issues, the achievement of climate and biodiversity targets may be jeopardized by further disruption of ecosystem functioning with negative socioeconomic issues to humankind: the marine carbon cycle is the most critical dimension of the biophysical system directly and immediately affecting human wellbeing via the provision of ecosystem goods and services. More basic research is key to define the area and the timing for management action impacting the marine carbon cycle, operative at national or regional scales with global impacts.

Author Contributions: Conceptualization L.B. and P.F.-F.; methodology L.B.; P.F.-F. and L.O., software, L.B.; validation, L.B., P.F.-F., A.C., D.C., M.M.d.M., M.G., Y.M., O.G. and L.O.; formal analysis, L.B., P.F.-F., A.C., D.C., M.M.d.M., M.G., Y.M., O.G. and L.O.; investigation, L.B., P.F.-F., A.C., D.C., M.M.d.M., M.G., Y.M., O.G. and L.O.; resources, L.B.; data curation L.B., P.F.-F., A.C., D.C., M.M.d.M., M.G., Y.M., O.G. and L.O.; writing—original draft preparation, L.B., P.F.-F. and L.O.; writing—review and editing, L.B., P.F.-F., A.C., D.C., M.M.d.M., M.G., Y.M., O.G. and L.O.; visualization, L.B., P.F.-F.; supervision, L.B. All authors have read and agreed to the published version of the manuscript.

Funding: Sector Commission for Scientific Research (CSIC), Universidad de la República by founding the Project I + D/2014 “Analysis of the coupling of oceanographic processes for the management of marine space in a region of high productivity in the Uruguayan Exclusive Economic Zone—Southwest Atlantic”.

Institutional Review Board Statement: Not applicable.

Informed Consent Statement: Not applicable.

Data Availability Statement: Data sharing not applicable. No new data were created or analyzed in this study. Data sharing is not applicable to this article.

Acknowledgments: Acknowledgements are due to the Sector Commission for Scientific Research (CSIC) Universidad de la República by founding the Project I + D/2014 “Analysis of the coupling of oceanographic processes for the management of marine space in a region of high productivity in the Uruguayan Exclusive Economic Zone—Southwest Atlantic”. Guillermo Burone is acknowledged for the artwork of Figures 2, 6a–c and 7a–c. This work was part of the Ph.D. Thesis of YM (PEDECIBA). This paper is publication N°7 of the Grupo de Trabajo en Ciencia y Tecnología Marina (CINCYTEMA), IECA, Facultad de Ciencias, UdelaR.

Conflicts of Interest: The authors declare no conflict of interest

Abbreviations

AABW	Antarctic Bottom Water
AAIW	Antarctic Intermediate Water
AAIW _r	Recirculated Antarctic Intermediate Water
BC	Brazil Current
BeC	Benguela Current
BMC	Brazil-Malvinas Confluence
CDS	Contouritic Depositional System
C _{org}	Organic Carbon
CM	Conceptual models
C/N	Carbon-Nitrogen rate
DIC	Dissolved organic carbon
DIEA	Office of Agricultural Statistics
DIN	Dissolved Inorganic Nitrogen
DOM	Dissolved Organic Matter
ENSO	El Niño Southern Oscillation
GDP	Gross Domestic Product
INL	Intermediate Nepheloids Layers
J _z	Organic Carbon Flux
LCDW	Lower Circumpolar Deep Water
LMEs	Large Marine Ecosystems
MC	Malvinas Current
MPAs	Marine Protected Areas
NADW	North Atlantic Deep Water
NEOW	Marine Ecoregions of the World
PP	Primary Productivity
PPOW	Pelagic Provinces of the World
RdIP	Río de la Plata
SACZ	South Atlantic Convergence Zone
SACW	South Atlantic Central Water
SAW	Subantarctic Water STSW
SWAO	South West Atlantic Ocean
SCS	Submarine Canyons System
STSF	Subtropical Shelf Water
TW	Tropical Water
UCDW	Upper Circumpolar Deep Water
UCM	Uruguayan Continental Margin

References

1. Lowe, D.R. Sediment gravity flows: Their classification and some problems of application to natural flows and deposits. *Geol. Cont. Slopes* **1979**, *75–82*. [[CrossRef](#)]
2. Menot, L.; Sibuet, M.; Carney, R.S.; Levin, L.A.; Rowe, G.T.; Billett, D.S.M.; Poore, G.; Kitazato, H.; Vanreusel, A.; Galéron, J.; et al. New Perceptions of Continental Margin Biodiversity. In *Life World's Ocean Divers Distrib Abundance*; Wiley: Hoboken, NJ, USA, 2010; pp. 79–102.
3. DeMaster, D.J.; Thomas, C.J.; Blair, N.E.; Fornes, W.L.; Plaia, G.; Levin, L.A. Deposition of bomb 14C in continental slope sediments of the Mid-Atlantic Bight: Assessing organic matter sources and burial rates. *Deep. Res. Part II Top. Stud. Oceanogr.* **2002**, *49*, 4667–4685. [[CrossRef](#)]

4. Hartnett, H.E.; Keil, R.G.; Hedges, J.I.; Devol, A.H. Influence of oxygen exposure time on organic carbon preservation in continental margin sediments. *Nature* **1998**, *391*, 572–575. [CrossRef]
5. Wefer, G.; Billet, D.; Hebbeln, D.; Jorgensen, B.B.; Schlüter, M.; Weering, T.C.E.V. *Ocean Margin Systems*; Springer: Berlin/Heidelberg, Germany, 2003; p. 495.
6. Falkowski, P.; Scholes, R.J.; Boyle, E.; Canadell, J.; Canfield, D.; Elser, J.; Gruber, N.; Hibbard, K.; Hogberg, P.; Linder, S.; et al. The global carbon cycle: A test of our knowledge of earth as a system. *Science* **2000**, *290*, 291–296. [CrossRef]
7. Muller-Karger, F.E.; Varela, R.; Thunell, R.; Luerssen, R.; Hu, C.; Walsh, J.J. The importance of continental margins in the global carbon cycle. *Geophys. Res. Lett.* **2005**, *32*, 1–4. [CrossRef]
8. Laruelle, G.G.; Cai, W.J.; Hu, X.; Gruber, N.; Mackenzie, F.T.; Regnier, P. Continental shelves as a variable but increasing global sink for atmospheric carbon dioxide. *Nat. Commun.* **2018**, *9*, 454. [CrossRef] [PubMed]
9. Wefer, G.; Berger, W.H.; Behre, K.-E.; Jansen, E. (Eds.) *Climate Development and History of the North Atlantic Realm*; Springer: Berlin/Heidelberg, Germany, 2002; ISBN 978-3-642-07744-9.
10. Wollast, R. Continental Margins—Review of Geochemical Settings. In *Ocean Margin Systems*; Springer: Berlin/Heidelberg, Germany, 2002; pp. 15–31.
11. Liu, K.-K.; Atkinson, L.; Quiñones, R.A.; Talaue-McManus, L. Biogeochemistry of Continental Margins in a Global Context. In *Carbon and Nutrient Fluxes in Continental Margins*; Springer: Berlin/Heidelberg, Germany, 2010; pp. 3–24.
12. Chen, S.P.; van Genderen, J. Digital Earth in support of global change research. *Int. J. Digit. Earth* **2008**, *1*, 43–65. [CrossRef]
13. Borús, J.; Uriburu Quirno, M.; Calvo, D. *Evaluación de Caudales Diarios Descargados por los Grandes Ríos del Sistema del Plata al Estuario del Río de la Plata*; Dirección de Sistemas de Información y Alerta Hidrológico: Buenos Aires, Argentina, 2017.
14. Hoffmeyer, M.S.; Sabatini, M.E.; Brandini, F.P.; Calliari, D.L.; Santinelli, N.H. (Eds.) *Plankton Ecology of the Southwestern Atlantic*; Springer International Publishing: Cham, Switzerland, 2018; ISBN 978-3-319-77868-6.
15. Field, C.B. Primary Production of the Biosphere: Integrating Terrestrial and Oceanic Components. *Science* **1998**, *281*, 237–240. [CrossRef] [PubMed]
16. Acha, E.M.; Mianzan, H.W.; Guerrero, R.A.; Favero, M.; Bava, J. Marine fronts at the continental shelves of austral South America: Physical and ecological processes. *J. Mar. Syst.* **2004**, *44*, 83–105. [CrossRef]
17. Acha, E.M.; Piola, A.; Iribarne, O.; Mianzan, H. *Ecological Processes at Marine Fronts Oases in the Ocean*; Springer International Publishing: Cham, Switzerland, 2015; 68p, ISBN 9783319154787.
18. Piola, A.R.; Campos, E.J.D.; Möller, O.O., Jr.; Charo, M.; Martínez, C. Title: Subtropical shelf front off eastern South America. *J. Geophys. Res. Ocean.* **2000**, *105*, 6565–6578. [CrossRef]
19. Ortega, L.; Martínez, A. Multiannual and seasonal variability of water masses and fronts over the Uruguayan shelf. *J. Coast. Res.* **2007**, *23*, 618–629. [CrossRef]
20. Urien, C.M.; Ewing, M. Recent Sediments and Environments of Southern Brazil, Uruguay, Buenos Aires and Río Negro Continental Shelf. In *The Geology of Continental Margins*; Burk, C., Drake, C.H., Eds.; Springer: New York, NY, USA, 1974; pp. 157–177.
21. Burone, L.; Franco-Fraguas, P.; Mahiques, M.; Ortega, L. Geomorphological and Sedimentological Characterization of the Uruguayan Continental Margin: A Review and State of Art. *J. Sediment. Environ.* **2018**, *3*, 253–264. [CrossRef]
22. Burone, L.; Franco-Fraguas, P.; de Mahiques, M.M.; Lahuerta, N.; de Rada, J.R.D.; Rodríguez, M.; Bicego, M.C.; Marín, Y.; Gómez-Erache, M.; Ortega, L. the Imprint of the Geological Inheritance and Present Dynamics on Uruguayan Inner Shelf Sediments (South-Western Atlantic). *J. Sediment. Environ.* **2019**, *4*, 403–420. [CrossRef]
23. Hernández-Molina, F.J.; Soto, M.; Piola, A.R.; Tomasini, J.; Preu, B.; Thompson, P.; Badalini, G.; Creaser, A.; Violante, R.A.; Morales, E.; et al. A contourite depositional system along the Uruguayan continental margin: Sedimentary, oceanographic and paleoceanographic implications. *Mar. Geol.* **2016**, *378*, 333–349. [CrossRef]
24. Lantzsch, H.; Hanebuth, T.J.J.; Chiessi, C.M.; Schwenk, T.; Violante, R.A. The high-supply, current-dominated continental margin of southeastern South America during the late quaternary. *Quat. Res.* **2014**, *81*, 339–354. [CrossRef]
25. Barreiro, M.; Martínez, A.; Ortega, L.; Rabellino, J. Hidrodinámica. In *Uruguay, Mar Territorial/Programa Oceanográfico de Caracterización del Margen Continental de la República Oriental del Uruguay*; ANCAP: Montevideo, Uruguay, 2014; pp. 25–61, ISBN 978-9974-8465-1-7.
26. Burone, L.; Centurión, V.; Cibilis, L.; Franco-Fraguas, P.; García-Rodríguez, F.; García, G.; Pérez, L. Sedimentología y Paleooceanografía. In *Uruguay, Mar Territorial/Programa Oceanográfico de Caracterización del Margen Continental de la República Oriental del Uruguay*; ANCAP: Montevideo, Uruguay, 2014; pp. 54–56. ISBN 978-9974-8465-1-7.
27. Marín, Y.; Chocca, J.; González, B.; Beathate, G. Interacción entre diferentes actividades antrópicas. In *Uruguay, Mar Territorial/Programa Oceanográfico de Caracterización del Margen Continental de la República Oriental del Uruguay*; ANCAP: Montevideo, Uruguay, 2014; pp. 343–368. ISBN 978-9974-8465-1-7.
28. Manley, P.N.; Zielinski, W.J.; Stuart, C.M.; Keane, J.J.; Lind, A.J.; Brown, C.; Plymale, B.L.; Napper, C.O. Monitoring Ecosystems in the Sierra Nevada: The Conceptual Model Foundation. *Environ. Monit. Assess.* **2000**, *64*, 139–152. [CrossRef]
29. Launer, R.L.; Wilkinson, G.N. *Robustness in Statistics*; Wilkinson, R.L.L.G.N., Academy, L., Eds.; Elsevier Inc.: Amsterdam, The Netherlands, 1979; 312p, ISBN 9781483263366.
30. Gross, J.E. Developing Conceptual Models for Monitoring Program. Available online: http://science.nature.nps.gov/im/monitor/docs/Conceptual_Modelling.pdf (accessed on 5 March 2021).

31. Stramma, L.; England, M. On the water masses and mean circulation of the South Atlantic Ocean. *J. Geophys. Res. Ocean.* **1999**, *104*, 20863–20883. [[CrossRef](#)]
32. Garzoli, S.L. Geostrophic velocity and transport variability in the Brazil-Malvinas Confluence. *Deep. Res. Part I* **1993**, *40*, 1379–1403. [[CrossRef](#)]
33. Stramma, L.; Peterson, R.G. The south-Atlantic current. *J. Phys. Oceanogr.* **1990**, *20*, 846–859. [[CrossRef](#)]
34. Goni, G.J.; Bringas, F.; Dinezio, P.N. Observed low frequency variability of the Brazil Current front. *J. Geophys. Res. Ocean.* **2011**, *116*, 1–10. [[CrossRef](#)]
35. Peterson, R.G.; Stramma, L. Upper-level circulation in the South Atlantic Ocean. *Prog. Oceanogr.* **1991**, *26*, 1–73. [[CrossRef](#)]
36. Sverdrup, H.U.; Johnson, M.V.; Fleming, R. *The Oceans, Their Physical Chemistry and General Biology*; Prentice-Hall: New York, NY, USA, 1942; 1087p.
37. Provost, C.C.; Escoffier, K.; Maamaatuaiahutapu, A.; Kartavtseff, V.G. Subtropical mode waters in the South Atlantic Ocean. *J. Geophys. Res.* **1999**, *104*, 21033–21049. [[CrossRef](#)]
38. Barreiro, M.; Sitz, L.; de Mello, S.; Franco, R.F.; Renom, M.; Farneti, R. Modelling the role of Atlantic air–sea interaction in the impact of Madden–Julian Oscillation on South American climate. *Int. J. Climatol.* **2019**, *39*, 1104–1116. [[CrossRef](#)]
39. Piola, A.R.; Matano, R.P.; Palma, E.D.; Möller, O.O.; Campos, E.J.D. The influence of the Plata River discharge on the western South Atlantic shelf. *Geophys. Res. Lett.* **2005**, *32*, 1–4. [[CrossRef](#)]
40. Guerrero, R.A.; Piola, A.R.; Fenco, H.; Matano, R.P.; Combes, V.; Chao, Y.; James, C.; Palma, E.D.; Saraceno, M.; Strub, P.T.; et al. The salinity signature of the cross-shelf exchanges in the Southwestern Atlantic Ocean: Numerical simulations. *J. Geophys. Res. Oceans Southwest. Atl. Ocean Satell. Obs.* **2014**, *1*, 1–17.
41. Ciotti, Á.M.; Odebrecht, C.; Fillmann, G.; Moller, O.O. Freshwater outflow and Subtropical Convergence influence on phytoplankton biomass on the southern Brazilian continental shelf. *Cont. Shelf Res.* **1995**, *15*, 1737–1756. [[CrossRef](#)]
42. Piola, A.R.; Möller, O.O.; Guerrero, R.A.; Campos, E.J.D. Variability of the subtropical shelf front off eastern South America: Winter 2003 and summer 2004. *Cont. Shelf Res.* **2008**, *28*, 1639–1648. [[CrossRef](#)]
43. Machado, I.; Barreiro, M.; Calliari, D. Variability of chlorophyll-a in the Southwestern Atlantic from satellite images: Seasonal cycle and ENSO influences. *Cont. Shelf Res.* **2013**, *53*, 102–109. [[CrossRef](#)]
44. Acha, E.M.; Simionato, C.G.; Carozza, C.M.H. Climate-induced year-class fluctuations of whitemouth croaker *Micropogonias furnieri* (Pisces, Sciaenidae) in the Río de la Plata estuary, Argentina–Uruguay. *Fish Ocean.* **2012**, *21*, 58–77. [[CrossRef](#)]
45. Franco, B.C.; Defeo, O.; Piola, A.R.; Barreiro, M.; Yang, H.; Ortega, L.; Gianelli, I.; Castello, J.P.; Vera, C.; Buratti, C.; et al. Climate change impacts on the atmospheric circulation, ocean, and fisheries in the southwest South Atlantic Ocean: A review. *Clim. Chang.* **2020**, *162*, 2359–2377. [[CrossRef](#)]
46. Möller, O.O.; Piola, A.R.; Freitas, A.C.; Campos, E.J.D. The effects of river discharge and seasonal winds on the shelf off southeastern South America. *Cont. Shelf Res.* **2008**, *28*, 1607–1624. [[CrossRef](#)]
47. Hinz, K.; Neben, S.; Schreckenberger, B.; Roeser, H.; Block, M.; De Souza, K.; Meyer, H. The Argentine continental margin north of 48°S: Sedimentary successions, volcanic activity during breakup. *Mar. Pet. Geol.* **1996**, *16*, 1–25. [[CrossRef](#)]
48. Franke, D.; Neben, S.; Ladage, S.; Schreckenberger, B.; Hinz, K. Margin segmentation and volcano-tectonic architecture along the volcanic margin off Argentina/Uruguay, South Atlantic. *Mar. Geol.* **2007**, *244*, 46–67. [[CrossRef](#)]
49. Soto, M.; Morales, E.; Veroslavsky, G.; de Santa Ana, H.; Ucha, N.; Rodríguez, P. The continental margin of ur: Crustal architecture and segmentation. *Mar. Pet. Geol.* **2011**, *28*, 1676–1689. [[CrossRef](#)]
50. Hueck, M.; Oriolo, S.; Dunkl, I.; Wemmer, K.; Oyhantçabal, P.; Schanofski, M.; Basei, M.Á.S.; Siegesmund, S. Phanerozoic low-temperature evolution of the Uruguayan Shield along the South American passive margin. *J. Geol. Soc.* **2017**, *174*, 609–626. [[CrossRef](#)]
51. Panario, D.; Gutiérrez, O.; Sánchez Bettucci, L.; Peel, E.; Oyhantçabal, P.; Rabassa, J. Ancient Landscapes of Uruguay. In *Gondwana Landscapes in southern South America*; Springer: Dordrecht, The Netherlands, 2014; pp. 161–199.
52. Urien, C.M.; Martins, L.R. *Sedimentación marina en América del Sur Oriental. Sobre Ecología Bentónica y Sedimentación de la Plataforma Continental del Atlántico Sur. Parte 1: Geología y Sedimentación*; Memorias del Seminario: Porto Alegre, Brazil, 1979.
53. Urien, C.M.; Martins, L.R.; Martins, I.R. *Evolução Geológica do Quaternario do Litoral Atlântico Uruguaio, Plataforma Continental e Regiões Vizinhas*; Memorias del Seminario: Porto Alegre, Brazil, 1980.
54. Urien, C.M.; Martins, L.R.; Martins, I.R. *Modelos Depositionais na Plataforma Continental do Rio Grande do Sul (Brasil)*; AGIRS: Buenos Aires, Argentina, 1980.
55. Morales, E.; Chang, H.K.; Soto, M.; Corrêa, F.S. Tectonic and Stratigraphic Evolution of the Punta del Este and Pelotas Basins Tectonic and Stratigraphic Evolution of the Punta del Este and Pelotas Basins (offshore Uruguay). *Pet. Geosci.* **2017**, *23*, 415. [[CrossRef](#)]
56. Muñoz, A.; Fontan, A.; Marin, Y.; Carranza, A.; Franco-Fraguas, P.; Rubio, L. Informe de Campaña Uruguay 0110. In *Buque de Investigación Oceanográfica Miguel Oliver (SGM)*; DINARA: Montevideo, Uruguay, 1995.
57. Urien, C.M.; Ewing, M. Recent sediments and environments of Southern Brazil, Uruguay, Buenos Aires and Río Negro continental Shelf. In *The Geology of Continental Margins, IV. Recent Sedimentation*; Burk, C.A., Drake, C.L., Eds.; Springer: Berlin/Heidelberg, Germany, 1974; pp. 157–177.
58. Cavallotto, J.L.; Violante, R.A.; Colombo, F. Evolución y cambios ambientales de la llanura costera de la cabecera del río de la Plata. *Rev. Asoc. Geol. Argent.* **2005**, *60*, 353–367.

59. Urien, C.M.; Ottman, F. Historie du Rio de la Plata au Quaternaire. *Quaternaria* **1971**, *XIV*, 51–59.
60. Parker, G.; Violante, R.A.; Paterlini, C.M.; Costa, I.P.; Marcolini, S.I.; Cavallotto, J.L. Las Secuencias Depositacionales del plioceno-cuaternario en la plataforma submarina adyacente al litoral del Este Bonaerense. *Lat. Am. J. Sedimentol. Basin Anal.* **2008**, *15*, 105–124.
61. Violante, R.A.; Paterlini, C.M.; Costa, I.P.; Hernández-Molina, F.J.; Segovia, L.M.; Cavallotto, J.L.; Marcolini, S.; Bozzano, G.; Laprida, C. Sismoestratigrafía Y Evolución Geomorfológica. *Lat. Am. J. Sedimentol. Basin Anal.* **2010**, *17*, 33–62.
62. Violante, R.; Burone, L.; Mahiques, M.; Cavallotto, J.L. The Southeastern Atlantic Ocean: Present and Past. *Lat. Am. J. Sedimentol. Basin Anal.* **2017**, *24*, 2017.
63. Hernández-Molina, F.J.; Paterlini, M.; Violante, R.; Marshall, P.; de Isasi, M.; Somoza, L.; Rebesco, M. Contourite depositional system on the Argentine slope: An exceptional record of the influence of Antarctic water masses. *Geology* **2009**, *37*, 507–510. [[CrossRef](#)]
64. Lonardi, A.G.; Ewing, M. Sediment transport and distribution in the Argentine Basin. 4. Bathymetry of the continental margin, Argentine Basin and other related provinces. Canyons and sources of sediments. *Phys. Chem. Earth* **1971**, *8*, 81–121. [[CrossRef](#)]
65. Franco-Fraguas, P.; Burone, L.; Mahiques, M.; Ortega, L.; Urien, C.; Muñoz, A.; López, G.; Marin, Y.; Carranza, A.; Lahuerta, N.; et al. Hydrodynamic and geomorphological controls on surface sedimentation at the Subtropical Shelf Front/Brazil-Malvinas Confluence transition off Uruguay (Southwestern Atlantic Continental Margin). *Mar. Geol.* **2014**, *349*, 24–36. [[CrossRef](#)]
66. Franco-Fraguas, P.; Burone, L.; Goso, C.; Scarabino, F.; Muzio, R.; Carranza, A.; Ortega, L.; Muñoz, A.; Mahiques, M. Sedimentary processes in the head of the Cabo Polonio mega slide canyon (southwestern Atlantic margin off Uruguay) Sedimentary Processes in The Head of The Cabo Polonio Mega Slide Canyon (Southwestern Atlantic Margin Off Uruguay). *Lat. Am. J. Sedimentol. Basin Anal.* **2017**, *24*, 31–44.
67. Etchichury, M.C.; Remiro, J. La corriente de Malvinas y los sedimentos pampeano-patagónicos. *Rev. Mus. Argent. Cienc. Geológicas* **1963**, *1*, 1–11.
68. de Mahiques, M.M.; Tassinari, C.C.G.; Marcolini, S.; Violante, R.A.; Figueira, R.C.L.; da Silveira, I.C.A.; Burone, L.; de Mello e Sousa, S.H. Nd and Pb isotope signatures on the Southeastern South American upper margin: Implications for sediment transport and source rocks. *Mar. Geol.* **2008**, *250*, 51–63. [[CrossRef](#)]
69. Teruggi, M.E. El material volcánico-piroclástico en la sedimentación pampeana. *AAS Rev.* **1954**, *9*, 184–191.
70. Etchichury, M.C.; Remiro, J. Muestras de fondo de la plataforma continental comprendida entre los paralelos 34° y 36°30 de latitud sur y los meridianos 53°10 y 56°30 de longitud oeste. *VI Rev. Mus. Argent. Cienc. Nat. Bernardino Rivadavia* **1960**, *4*, 1–70.
71. Bozzano, G.; Violante, R.A.; Ceredo, M.E. Middle slope contourite deposits and associated sedimentary facies off NE Argentina. *Geo-Mar. Lett.* **2011**, *31*, 495–507. [[CrossRef](#)]
72. Krastel, S.; Wefer, G.; Hanebuth, T.J.J.; Antobreh, A.A.; Freudenthal, T.; Preu, B.; Schwenk, T.; Strasser, M.; Violante, R.; Winkelmann, D. Sediment dynamics and geohazards off Uruguay and the de la Plata River region (northern Argentina and Uruguay). *Geo-Mar. Lett.* **2011**, *31*, 271–283. [[CrossRef](#)]
73. Ai, F.; Strasser, M.; Preu, B.; Hanebuth, T.J.J.; Krastel, S.; Kopf, A. New constraints on oceanographic vs. seismic control on submarine landslide initiation: A geotechnical approach off Uruguay and northern Argentina. *Geo-Marine Lett.* **2014**, *34*, 399–417. [[CrossRef](#)]
74. Henkel, S.; Arnold, G.L.; Krastel, S.; Kasten, S. An interdisciplinary investigation of a recent submarine mass transport deposit at the continental margin off Uruguay. *Geochem. Geophys. Geosyst.* **2011**, *12*, 1–19. [[CrossRef](#)]
75. Bender, V.B. From Shelf Dynamics to Shelf Export: Evidences from Sedimentologic and Paleooceanographic Slope Record. Ph.D. Thesis, University of Bremen (Universität Bremen), Bremen, Germany, 2012. Available online: <http://nbn-resolving.de/urn:nbn:de:gbv:46-00102725-15> (accessed on 15 October 2020).
76. Frenz, M.; Höppner, R.; Stuut, J.-B.W.; Wagner, T.; Henrich, R. Surface Sediment Bulk Geochemistry and Grain-Size Composition Related to the Oceanic Circulation along the South American Continental Margin in the Southwest Atlantic. In *The South Atlantic in the Late Quaternary*; Springer: Berlin/Heidelberg, Germany, 2003; pp. 347–373.
77. Burone, L.; Ortega, L.; Franco-Fraguas, P.; Mahiques, M.; García-Rodríguez, F.; Venturini, N.; Marin, Y.; Brugnoli, E.; Nagai, R.; Muniz, P.; et al. A multiproxy study between the Río de la Plata and the adjacent South-western Atlantic inner shelf to assess the sediment footprint of river vs. marine influence. *Cont. Shelf Res.* **2013**, *55*, 141–154. [[CrossRef](#)]
78. Corrêa, I.C.S.; Zouain, R.N.A.; Weschenfelder, J.; Tomazelli, L.J. Áreas Fontes dos Minerais Pesados e sua Distribuição sobre a Plataforma Continental Sul-brasileira, Uruguai e Norte-argentina. *Pesqui. Geociências* **2008**, *35*, 137. [[CrossRef](#)]
79. López-Laborde, J. Distribución de sedimentos superficiales de fondo en el Río de la Plata exterior y plataforma adyacente. *Investig. Ocean.* **1987**, *1*, 19–30.
80. Martins, L.R.; Martins, I.R.; Urien, C.M. Aspectos Sedimentares da Plataforma Continental na Área de Influência do Rio de La Plata. *Gravel* **2003**, *1*, 68–80.
81. Campos, E.J.D.; Mulkherjee, S.; Piola, A.R.; de Carvalho, F.M.S. A note on a mineralogical analysis of the sediments associated with the Plata River and Patos Lagoon outflows. *Cont. Shelf Res.* **2008**, *28*, 1687–1691. [[CrossRef](#)]
82. De Mahiques, M.M.; Tessler, M.G.; Maria Ciotti, A.; Da Silveira, I.C.A.; E Sousa, S.H.D.M.; Figueira, R.C.L.; Tassinari, C.C.G.; Furtado, V.V.; Passos, R.F. Hydrodynamically driven patterns of recent sedimentation in the shelf and upper slope off Southeast Brazil. *Cont. Shelf Res.* **2004**, *24*, 1685–1697. [[CrossRef](#)]

83. Burone, L.; de e Sousa, S.H.M.; de Mahiques, M.M.; Valente, P.; Ciotti, A.; Yamashita, C. Benthic foraminiferal distribution on the southeastern Brazilian shelf and upper slope. *Mar. Biol.* **2011**, *158*, 159–179. [[CrossRef](#)]
84. MIX, A.C. Influence of Productivity Variations on Long-Term Atmospheric Co₂. *Nature* **1989**, *337*, 541–544. [[CrossRef](#)]
85. Altenbach, A.B.; Sarnthein, M. Productivity record in benthic foraminifera. In *Productivity of the Ocean: Present and Past*; Berger, W.H., Smetacek, V.S., Wefer, G., Eds.; Report on the Dahlem Workshop on Productivity of the Oceans; Springer: Berlin, Germany, 1988.
86. Altenbach, A.V. Short term processes and patterns in the foraminiferal response to organic flux rates. *Mar. Micropaleontol.* **1992**, *19*, 119–129. [[CrossRef](#)]
87. Gage, J.D. Benthic Secondary Production in the Deep Sea. In *Deep-Sea Food Chains and the Global Carbon Cycle*; Springer: Dordrecht, The Netherlands, 1992; pp. 199–216.
88. Herguera, J.C.; Berger, W.H. Paleoproductivity from benthic foraminifera abundance: Glacial to postglacial change in the west-equatorial Pacific. *Geology* **1991**, *19*, 1173. [[CrossRef](#)]
89. Linke, P.; Altenbach, A.V.; Graf, G.; Heeger, T. Response of deep-sea benthic foraminifera to a simulated sedimentation event. *J. Foraminifer. Res.* **1995**, *25*, 75–82. [[CrossRef](#)]
90. Loubere, P. The surface ocean productivity and bottom water oxygen signals in deep water benthic foraminiferal assemblages. *Mar. Micropaleontol.* **1996**, *28*, 247–261. [[CrossRef](#)]
91. Fariduddin, M.; Loubere, P. The surface ocean productivity response of deeper water benthic foraminifera in the Atlantic Ocean. *Mar. Micropaleontol.* **1997**, *32*, 289–310. [[CrossRef](#)]
92. Burone, L.; Pires-vanin, A.N.A.M.S. Foraminiferal assemblages in Ubatuba Bay, south-eastern Brazilian coast. *Sci. Mar.* **2006**, *70*, 203–217. [[CrossRef](#)]
93. Burone, L.; Venturini, N.; Sprechmann, P.; Valente, P.; Muniz, P. Foraminiferal responses to polluted sediments in the Montevideo coastal zone, Uruguay. *Mar. Pollut. Bull.* **2006**, *52*, 61–73. [[CrossRef](#)] [[PubMed](#)]
94. Burone, L.; Valente, P.; Maria, A.N.A.; Sousa, H.D.E.M.E.; Mahiques, M.M.; Braga, E. Benthic foraminiferal variability on a monthly scale in a subtropical bay moderately affected by urban sewage. *Sci. Mar.* **2007**, *71*, 775–792. [[CrossRef](#)]
95. de Mello, C.; Burone, L.; Ortega, L.; Franco-Fraguas, P.; Lahuerta, N.; Mahiques, M.; Marin, Y. Benthic foraminiferal distributions on the Uruguayan continental margin (South-western Atlantic) and controlling environmental factors. *Cont. Shelf Res.* **2014**, *91*, 120–133. [[CrossRef](#)]
96. Calliari, D.; Brugnoli, E.; Ferrari, G.; Vizziano, D. Phytoplankton distribution and production along a wide environmental gradient in the South-West Atlantic off Uruguay. *Hydrobiologia* **2009**, *620*, 47–61. [[CrossRef](#)]
97. Lutz, V.; Segura, V.; Dogliotti, A.; Tavano, V.; Brandini, F.P.; Calliari, D.L.; Ciotti, A.M.; Villafaña, V.F.; Schloss, I.R.; Corrêa, F.M.P.S.; et al. Overview on Primary Production in the Southwestern Atlantic. In *Plankton Ecology of the Southwestern Atlantic*; Springer International Publishing: Cham, Switzerland, 2018; pp. 101–126.
98. Dogliotti, A.I.; Ruddick, K.; Guerrero, R. Seasonal and inter-annual turbidity variability in the Río de la Plata from 15 years of MODIS: El Niño dilution effect. *Estuar. Coast. Shelf Sci.* **2016**, *182*, 27–39. [[CrossRef](#)]
99. Cazarré, M.E. *Comparación de la Impronta Sedimentar y Distribución de Foraminíferos Bajo Condiciones Hidrodinámicas Contrastantes en el Margen Continental Uruguayo*; Universidad de la República: Montevideo, Uruguay, 2020.
100. Rodríguez, M. Caracterización Biogeoquímica del Margen Continental Uruguayo en un Perfil Batimétrico Entre los 29 y 3800 m de Profundidad (Atlántico Sudoccidental). Ph.D. Thesis, Universidad de la República, Montevideo, Uruguay, 2020.
101. Gutiérrez, N.D.O. Development of a new scallop *Zygochlamys patagonica* fishery in Uruguay: Latitudinal and bathymetric patterns in biomass and population structure. *Fish. Res.* **2003**, *62*, 21–36. [[CrossRef](#)]
102. Gayoso, A.M.; Podestd, G.P. Surface hydrography and phytoplankton of the Brazil-Malvinas currents confluence. *J. Plankton Res.* **1986**, *18*, 941–951. [[CrossRef](#)]
103. Brandini, F.P.; Boltovskoyby, D.; Piolad, A.; Kocmurb, S.; Riittgkrs, R.; Abreug, P.C.; Lopes, R.M. Multiannual trends in fronts and distribution of nutrients and chlorophyll in the southwestern Atlantic (30–62' S). *Deep Sea Res. Part I Oceanogr. Res. Pap.* **2000**, *47*, 1015–1033.
104. Saraceno, M.; Provost, C.; Piola, A.R. On the relationship between satellite-retrieved surface temperature fronts and chlorophyll a in the western South Atlantic. *J. Geophys. Res.* **2005**, *110*, C11016. [[CrossRef](#)]
105. Franco-Fraguas, P.; Burone, L.; Mahiques, M.; Ortega, L.; Carranza, A. Modern sedimentary dynamics in the Southwestern Atlantic Contouritic Depositional System: New insights from the Uruguayan margin based on a geochemical approach. *Mar. Geol.* **2016**, *376*, 15–25. [[CrossRef](#)]
106. Cibilis, L. *Productividad Marina en el Margen Continental Uruguayo-Atlántico Suroccidental. un Análisis Multiproxie*, Facultad de Ciencias; Universidad de la República: Montevideo, Uruguay, 2016.
107. Calbet, A.; Landry, M.R. Phytoplankton growth, microzooplankton grazing, and carbon cycling in marine systems. *Limnol. Oceanogr.* **2004**, *49*, 51–57. [[CrossRef](#)]
108. Behrenfeld, M.J.; Boss, E.S. Student's tutorial on bloom hypotheses in the context of phytoplankton annual cycles. *Glob. Chang. Biol.* **2018**, *24*, 55–77. [[CrossRef](#)]
109. Scarabino, F.; Zelaya, D.G.; Orensanz, J.L.; Ortega, L.; Defeo, O.; Schwindt, E.; Carranza, A.; Zaffaroni, J.C.; Martínez, G.; Scarabino, V.; et al. Cold, Warm, Temperate and Brackish: Bivalve Biodiversity in a Complex Oceanographic Scenario (Uruguay, Southwestern Atlantic). *Am. Malacol. Bull.* **2015**, *33*, 284. [[CrossRef](#)]

110. Garcia, V.M.T.; Garcia, C.A.E.; Mata, M.M.; Pollery, R.C.; Piola, A.R.; Signorini, S.R.; McClain, C.R.; Iglesias-Rodriguez, M.D. Environmental factors controlling the phytoplankton blooms at the Patagonia shelf-break in spring. *Deep Sea Res. Part I Oceanogr. Res. Pap.* **2008**, *55*, 1150–1166. [[CrossRef](#)]
111. Lahuerta, N. Determinação Do Grau Da Influência Terrestre Versus Marinha Ao Longo Da Transição Río De La Plata—Oceano Atlantico Sul, Através De Proxies Bióticos E Abióticos. Master's Thesis, Universidade de Sao Paulo, Sao Paulo, Brazil, 2014.
112. Tyson, R. *Sedimentary Organic Matter. Organic Facies and Palynofacies*; Springer: Berlin/Heidelberg, Germany, 1995.
113. Freplata. *Análisis Diagnóstico Transfronterizo del Río de la Plata y su Frente Marítimo. Documento Técnico. Proyecto "Protección Ambiental del Río de la Plata y su Frente Marítimo: Prevención y Control de la Contaminación y Restauración de Hábitats"*; Proyecto PNUD; PNUD: Montevideo, Uruguay, 2004; 668p.
114. Conde, M.R.R. (Ed.) *Bases Para la Conservación y el Manejo de la Costa Uruguaya*; Vida Silvestre: Montevideo, Uruguay, 2006.
115. Gómez-Erache, M.; Martino, D.; Defeo, O.; Vincent, P.; Acuña, A.; Amestoy, F.; De Álava, A.; Castiñeira, E.; Delfino, E.; Fagúndez, C.; et al. Zona Costera. In *Geo Uruguay. El Estado del Medio Ambiente en Uruguay*; PNUMA-CLAES-DINAMA: Montevideo, Uruguay, 2008; pp. 118–176.
116. Gutiérrez, O.; Panario, D. Caracterización y dinámica de la costa uruguaya, una revisión. In *Ciencias Marino-Costeras en el Umbral del Siglo XXI, desafíos en Latinoamérica y el Caribe*; Muniz, P., Conde, D., Venturini, N., Brugnoli, E., Eds.; Editorial AGT S.A: México DF, Mexico, 2019; pp. 61–91.
117. Framiñan, M.B.; Brown, O.B. Study of the Rio de la Plata turbidity front. Part I: Spatial and temporal distribution. *Cont. Shelf Res.* **1996**, *16*, 1259–1267. [[CrossRef](#)]
118. Barros, V. *Escenarios Hidrológicos de Caudales Medios del río Paraná y Uruguay*; Unidas, N., Ed.; CEPAL: Santiago, Chile, 2013; ISBN 1564418. Available online: <http://hdl.handle.net/11362/5696> (accessed on 20 October 2020).
119. Guerrero, R.A.; Acha, E.M.; Framiñan, M.B.; Lasta, C.A. Physical oceanography of the Río de la Plata Estuary, Argentina. *Cont. Shelf Res.* **1997**, *17*, 727–742. [[CrossRef](#)]
120. Nagy, G.J.; Gómez-Erache, M.; López, C.H.; Perdomo, A.C. Distribution patterns of nutrients and symptoms of eutrophications in the Rio de la Plata estuary. *Hifrobiología* **2002**, *475–476*, 125–139. [[CrossRef](#)]
121. Panario, D.; Gutiérrez, O. Introducción a la geomorfología de lagunas costeras, lagos someros y charcas de Uruguay. In *El Holoceno en la Zona Costera de Uruguay*; García-Rodríguez, F., Ed.; Ediciones Universitarias, Comisión Sectorial de Investigación Científica (CSIC); Udelar: Montevideo, Uruguay, 2011; pp. 49–63.
122. Nagy, G.J.; López-Laborde, J.; Anastasia, L. Zonación ambiental del Río de La Plata exterior: Salinidad y Turbiedad. *Investgaciones Ocean.* **1987**, *1*, 31–56.
123. Panario, D.; Gutierrez, O. Dinámica y fuentes de sedimentos de las playas uruguayas. In *Bases Para la Conservación y el Manejo de la Costa Uruguaya*; Menafrá, R., Rodríguez-Gallego, L., Scarabino, F., Conde, D., Eds.; VIDA SILVESTRE: Montevideo, Uruguay, 2006; p. 688.
124. Windom, H.L.; Moore, W.S.; Niencheski, L.F.H.; Jahnke, R.A. Submarine groundwater discharge: A large, previously unrecognized source of dissolved iron to the South Atlantic Ocean. *Mar. Chem.* **2006**, *102*, 252–266. [[CrossRef](#)]
125. Niencheski, L.F.H.; Windom, H.L.; Moore, W.S.; Jahnke, R.A. Submarine groundwater discharge of nutrients to the ocean along a coastal lagoon barrier, southern Brazil. *Mar. Chem.* **2007**, *106*, 546–561. [[CrossRef](#)]
126. Paiva, M.; Niencheski, F.H. Advances of Submarine Groundwater Discharge Studies in South America. *J. Braz. Chem. Soc.* **2017**, *29*, 916–924. [[CrossRef](#)]
127. Calliari, D.L.; Gómez-Erache, M.; Cantonnet, D.V.; Alonso, C. Near-Surface Biogeochemistry and Phytoplankton Carbon Assimilation in the Near-Surface Biogeochemistry and Phytoplankton Carbon Assimilation in the Rio de la Plata Estuary. In *Plankton Ecology of the South West Atlantic Ocean: From the Subtropical to the Subantarctic Realm*; Hoffmeyer, M., Sabatini, M., Santinelli, N., Brandini, F., Calliari, D., Eds.; Springer: Cham, Switzerland, 2018; pp. 289–306.
128. Calliari, D.; Gómez-Erache, M.; Rodríguez-Graña, L.; Alonso, C.; Martínez, M.; Nogueira, L.; Espinosa, P. Plancton. In *Uruguay, Mar Territorial/Programa Oceanográfico de Caracterización del Margen Continental de la República Oriental del Uruguay*; ANCAP: Montevideo, Uruguay, 2014; pp. 25–61. ISBN 978-9974-8465-1.
129. Boltovskoy, D. *Atlas Del Zooplancton Del Atlántico Sudoccidental Y Métodos De Trabajo Con El Zooplancton Marino*; Boltovskoyby, D., Ed.; Publicación Especial INIDEP; INIDEP: Mar del Plata, Argentina, 1981.
130. Calliari, L.J.; Tozzi, H.A.M.; Klein, A.H.F. Beach morphology and coastline erosion associated with storm surge in Southern Brazil-Rio Grande to Chuí, RS. *An. Acad. Bras. Cienc.* **1998**, *70*, 231–247.
131. Parise, C.K.; Calliari, L.J.; Krusche, N. Extreme storm surges in the south of Brazil: Atmospheric conditions and shore erosion. *Brazilian. J. Oceanogr.* **2009**, *57*, 175–188. [[CrossRef](#)]
132. Gutiérrez, O.; Panario, D.; Nagy, G.J.; Bidegain, M.; Montes, C. Climate teleconnections and indicators of coastal systems response. *Ocean Coast. Manag.* **2016**, *122*, 64–76. [[CrossRef](#)]
133. MTOP/PNUD/UNESCO. *Conservación y Mejora de Playas-URU. 73.007*; PNUD: Montevideo, Uruguay, 1979.
134. Barboza, E.G.; Rosa, M.L.C.C.; Tomazelli, L.J.; Dillenburg, S.R.; Ayup- Zouain, R.N. *Problemática de los Ambientes Costeros. Sur de Brasil, Uruguay y Argentina*; López, R.Á., Marcomini, S.C., Eds.; Editorial Croquis: Buenos Aires, Argentina, 2011.
135. Simionato, C.G.; Clara Tejedor, M.L.; Campetella, C.; Guerrero, R.; Moreira, D. Patterns of sea surface temperature variability on seasonal to sub-annual scales at and offshore the Río de la Plata estuary. *Cont. Shelf Res.* **2010**, *30*, 1983–1997. [[CrossRef](#)]

136. Framiñan, M.B.; Etala, M.P.; Acha, E.M.; Guerrero, R.A.; Lasta, C.A.; Brown, O.B. *Estuaries of South America*; Springer: Berlin/Heidelberg, Germany, 1999.
137. Trinchin, R.; Ortega, L.; Barreiro, M. Spatiotemporal characterization of summer coastal upwelling events in Uruguay, South America. *Reg. Stud. Mar. Sci.* **2019**, *31*, 100787. [[CrossRef](#)]
138. Martínez, A.; Ortega, L. Delimitation of domains in the external Río de la Plata estuary, involving phytoplanktonic and hydrographic variables. *Braz. J. Oceanogr.* **2015**, *63*, 217–227. [[CrossRef](#)]
139. Rabellino, J. *Análisis Del Rol Del Frente Subtropical De Plataforma Sobre Huevos Y Larvas De Engraulis Anchoita Utilizando Un Enfoque Bio-Físico*; Universidad de la República: Montevideo, Uruguay, 2016.
140. Correa, S.I.C. BP: l' exemple de la plate-forme continentale du Rio Grande. *Marine Geology do.* **1996**, *130*, 163–178.
141. Gómez Pivel, M.A. A Costa Atlântica Uruguai Como um Sistema Geomorfológico. Master's Thesis, Universidad Federal de Rio Grande, Rio Grande, Brazil, 2001.
142. Matano, R.P.; Palma, E.D.; Piola, A.R. The influence of the Brazil and Malvinas Currents on the Southwestern Atlantic Shelf circulation. *Ocean Sci.* **2010**, *6*, 983–995. [[CrossRef](#)]
143. Depetris, P.J.; Griffin, J.J. Suspenden load in the Rio de la Plata basin. *Sedimentology* **1968**, *11*, 53–60. [[CrossRef](#)]
144. Cavallotto, J.L. Evolución holocena de la llanura costera del margen sur del Río de la Plata. *Rev. Asoc. Geol. Argent.* **2002**, *57*, 376–388.
145. Martins, L.R.; Urien, C.M. Areias da plataforma e a erosão costeira. *Gravel* **2004**, *2*, 4–24.
146. Razik, S.; Govin, A.; Chiessi, C.M.; von Dobeneck, T. Depositional provinces, dispersal, and origin of terrigenous sediments along the SE South American continental margin. *Mar. Geol.* **2015**, *363*, 261–272. [[CrossRef](#)]
147. Codignotto, J.O.; Dragani, W.C.; Martin, P.B.; Simionato, C.G.; Medina, R.A.; Alonso, G. Wind-wave climate change and increasing erosion in the outer Río de la Plata, Argentina. *Cont. Shelf Res.* **2012**, *38*, 110–116. [[CrossRef](#)]
148. Perez, L.; García-rodríguez, F.; Hanebuth, T.J.J. Variability in terrigenous sediment supply offshore of the Río de la Plata (Uruguay) recording the continental climatic history over the past 1200 years. *Clim. Past* **2016**, *1*, 623–634. [[CrossRef](#)]
149. Bender, V.B.; Hanebuth, T.J.J.; Chiessi, C.M. Holocene shifts of the Subtropical Shelf Front off southeastern South America controlled by high and low latitude atmospheric forcings. *Paleoceanography* **2013**, *28*, 481–490. [[CrossRef](#)]
150. Hanebuth, T.J.J.; Bender, V.B.; Nagai, R.H. Sediment Export Dynamics Reflecting The Holocene Hydrodynamic Variability Of A High-Energy Continental Shelf System (Southeastern South America). *J. Sediment. Environ.* **2019**, *4*, 312–331. [[CrossRef](#)]
151. Calliari, D.; Gómez, M.; Gómez, N. Biomass and composition of the phytoplankton in the Río de la Plata: Large-scale distribution and relationship with environmental variables during a spring cruise. *Cont. Shelf Res.* **2005**, *25*, 197–210. [[CrossRef](#)]
152. Panario, D. Dinámica de la costa Atlántica Uruguaya. In *Seminario: Costa Atlántica. Estado Actual del Conocimiento y Estrategia de Investigación Sobre la Dinámica de la Costa y Sus Barras Lagunares*; Hernández, J., Ed.; Probides: Rocha, Uruguay, 1999.
153. Kruk, C.; Martínez, A.; Nogueira, L.; Alonso, C.; Calliari, D. Morphological traits variability reflects light limitation of phytoplankton production in a highly productive subtropical estuary (Río de la Plata, South America). *Mar. Biol.* **2015**, *162*, 331–341. [[CrossRef](#)]
154. Gutiérrez, O.; Panario, D.; Nagy, G.J. Relationships between the Sand Cycle and The Behaviour of Small River Mouths: A Neglected Process/O Ciclo Da Areia E O Comportamento De Estuários De Rios Pequenos: Um Processo Negligenciado. *J. Sediment. Environ.* **2018**, *3*, 307–325. [[CrossRef](#)]
155. Niencheski, F.H.; Windom, H.L. Chemistry of a Surficial Aquifer of a Large Coastal Lagoon Barrier and its Relation to Adjacent Surface Waters of Brazil. *J. Coast. Res.* **2015**, *31*, 1417–1428. [[CrossRef](#)]
156. Carreto, J.; Negri, R.B.E. Algunas características del florecimiento del fitoplancton en el frente del Río de la Plata. *Rev. Investig. Desarro. Pesq.* **1986**, *29*, 7–29.
157. Vögler, R.; Arreguín-Sánchez, F.; Lercari, D.; del Monte-Luna, P.; Calliari, D. The effects of long-term climate variability on the trophodynamics of an estuarine ecosystem in southern South America. *Ecol. Model.* **2015**, *317*, 83–92. [[CrossRef](#)]
158. Negri, R.M.; Molinari, G.; Carignan, M.; Ortega, L.; Ruiz, M.G.; Cozzolino, E.; Cucchi-Colleoni, A.D.; Vivian Lutz, M.C.; García, A.; Izzo, S.; et al. Ambiente y Plancton en la Zona Común de Pesca Argentino-Uruguaya en un escenario de cambio climático. Publicación Com. Técnica Mix. *Frente Marítimo* **2014**, *24*, 251–316.
159. Scarabino, J.C.; Zaffaroni, C.; Clavijo, A.C.M.N. Bivalvos marinos y estuarinos de la costa uruguaya: Faunística, distribución, taxonomía y conservación. In *Bases Para la Conservación y el Manejo de la Costa Uruguaya*; Menafrá, R.L., Rodríguez-Gallego, F.S.C.D., Eds.; Vida Silvestre: Montevideo, Uruguay, 2006; pp. 157–169.
160. Carranza, A.; Defeo, O.; Beck, M. Diversity, conservation status and threats to native oysters (Ostreidae) around the Atlantic and Caribbean coasts of South America. *Aquat. Conserv. Mar. Freshw. Ecosyst.* **2009**, *19*, 344–353. [[CrossRef](#)]
161. Martos, P.; Piccolo, M.C. Hydrography of the Argentine continental shelf between 38° and 42° S. *Cont. Shelf Res.* **1988**, *8*, 1043–1056. [[CrossRef](#)]
162. Bisbal, G.A. The Southeast South American shelf large marine ecosystem. Evolution and components. *Mar. Policy* **1995**, *19*, 21–38. [[CrossRef](#)]
163. Maamaatuaiahutapu, K.V.; Garçon, C.; Provost, H.M. Transports of the Brazil and Malvinas currents at their confluence. *J. Mar. Res.* **1998**, *56*, 417–438. [[CrossRef](#)]

164. Preu, B.; Hernández-Molina, F.J.; Violante, R.; Piola, A.R.; Paterlini, C.M.; Schwenk, T.; Voigt, I.; Krastel, S.; Spiess, V. Morphosedimentary and hydrographic features of the northern Argentine margin: The interplay between erosive, depositional and gravitational processes and its conceptual implications. *Deep Sea Res. Part I Oceanogr. Res. Pap.* **2013**, *75*, 157–174. [[CrossRef](#)]
165. Cirano, M.; Mata, M.M.; Campos, E.J.; Deiró, N.F. A circulação oceânica de larga-escala na região oeste do Atlântico Sul com base no modelo de circulação Global OCCAM. *Rev. Bras. Geofísica* **2006**, *24*, 209–230. [[CrossRef](#)]
166. Johnson, G.C. Quantifying Antarctic Bottom Water and North Atlantic Deep Water volumes. *J. Geophys. Res.* **2008**, *113*, C05027. [[CrossRef](#)]
167. Purkey, S.G.; Johnson, G.C. Warming of Global Abyssal and Deep Southern Ocean Waters between the 1990s and 2000s: Contributions to Global Heat and Sea Level Rise Budgets. *J. Clim.* **2010**, *23*, 6336–6351. [[CrossRef](#)]
168. Voigt, I.; Henrich, R.; Preu, B.M.; Piola, A.R.; Hanebuth, T.J.J.; Schwenk, T.; Chiessi, C.M. A submarine canyon as a climate archive-Interaction of the antarctic intermediate water with the mar del plata canyon (southwest atlantic). *Mar. Geol.* **2013**, *341*, 46–57. [[CrossRef](#)]
169. Longhurst, A.R. *Ecological Geography of the Sea*; Elsevier Ltd.: Amsterdam, The Netherlands, 2001; ISBN 0124555594.
170. Boltovskoy, E. *South Atlantic Zooplankton*; Backhuys, Ed.; HOLANDA-PAISES BAJOS: Leiden, The Netherlands, 1999; ISBN 90-5782-035-8.
171. Saraceno, M.; Provost, C.; Piola, A.R.; Bava, J.; Gagliardini, A. Brazil Malvinas Frontal System as seen from 9 years of advanced very high resolution radiometer data. *J. Geophys. Res. C Ocean.* **2004**, *109*. [[CrossRef](#)]
172. Carranza, A.; Kitahara, M.; Scarabino, F.; Ortega, L.; Acosta, J.; Fontan, A.; Nacional, M.; Natural, D.H.; Science, M.; Genomics, C.; et al. Deep-Water Coral Reefs From the Uruguayan. *Building* **2012**, *42*, 411–414.
173. Spalding, M.D.; Fox, H.E.; Allen, G.R.; Davidson, N.; Ferdaña, Z.A.; Finlayson, M.; Halpern, B.S.; Jorge, M.A.; Lombana, A.; Lourie, S.A.; et al. Marine Ecoregions of the World: A Bioregionalization of Coastal and Shelf Areas. *Bioscience* **2007**, *57*, 573–583. [[CrossRef](#)]
174. Sherman, K. The Large Marine Ecosystem Approach for Assessment and Management of Ocean Coastal Waters. In *Sustaining Large Marine Ecosystems*; Hennessey, T.M., Sutinen, J.G., Eds.; Elsevier: Amsterdam, The Netherlands, 2005; pp. 3–16.
175. Spalding, M.D.; Agostini, V.N.; Rice, J.; Grant, S.M. Pelagic provinces of the world: A biogeographic classification of the world's surface pelagic waters. *Ocean Coast. Manag.* **2012**, *60*, 19–30. [[CrossRef](#)]
176. Marcelo Acha, E.; Mianzan, H.; Guerrero, R.; Carreto, J.; Giberto, D.; Montoya, N.; Carignan, M. An overview of physical and ecological processes in the Rio de la Plata Estuary. *Cont. Shelf Res.* **2008**, *28*, 1579–1588. [[CrossRef](#)]
177. Carranza, A.; Scarabino, F.; Ortega, L. Distribution of Large Benthic Gastropods in the Uruguayan Continental Shelf and Río de la Plata Estuary. *J. Coast. Res.* **2008**, *1*, 161–168. [[CrossRef](#)]
178. Giberto, D.A.; Bremec, C.S.; Acha, E.M.; Mianzan, H. Large-scale spatial patterns of benthic assemblages in the SW Atlantic: The Río de la Plata estuary and adjacent shelf waters. *Estuar. Coast. Shelf Sci.* **2004**, *61*, 1–13. [[CrossRef](#)]
179. Brazeiro, A.; Acha, E.; Mianzan, H.; Gómez, M.; Fernández, V. *Aquatic Priority Areas for the Conservation and Management of the Ecological Integrity of the Rio de la Plata and Its Maritime Front*; Technical Report PNUD Project/GEF RLA/99/G31; PNUD: Montevideo, Uruguay, 2003.
180. Gao, S.; Collins, M.B. Holocene sedimentary systems on continental shelves. *Mar. Geol.* **2014**, *352*, 268–294. [[CrossRef](#)]
181. Gao, S.; Collins, M.B.; Lanckneus, J.; De Moor, G.; Van Lancker, V. Grain size trends associated with net sediment transport patterns: An example from the Belgian continental shelf. *Mar. Geol.* **1994**, *121*, 171–185. [[CrossRef](#)]
182. Gao, S.; Collins, M. Net sediment transport patterns inferred from grain-size trends, based upon definition of “transport vectors”. *Sediment. Geol.* **1992**, *81*, 47–60. [[CrossRef](#)]
183. George, P. Allen Relationship between Grain Size Parameter Distribution and Current Patterns in the Gironde Estuary (France). *SEPM J. Sediment. Res.* **1971**, *41*, 74–88.
184. Stow, D.A.V.; Hernández-Molina, F.J.; Llave, E.; Sayago-Gil, M.; Díaz del Río, V.; Branson, A. Bedform-velocity matrix: The estimation of bottom current velocity from bedform observations. *Geology* **2009**, *37*, 327–330. [[CrossRef](#)]